REPORT DOCUMENTATION PAGE

Form Approved
OMB NO. 0704-0188

1. AGENCY USE ONLY (Leave blank)	2. REPORT DATE	3. REPORT TYPE AND DATES COVERED
	Sept 96	Final 20 Sep 93 - 19 Sep 95

4. TITLE AND SUBTITLE

SiC for High Power
Electro-optic Switching Application

5. FUNDING NUMBERS

DAAH04-93-2-0005

6. AUTHOR(S)

Michael G. Spencer and Senpeng Sheng

7. PERFORMING ORGANIZATION NAMES(S) AND ADDRESS(ES)

Howard University School of Engineering
2300 6th St. NW Washington, DC
20059

8. PERFORMING ORGANIZATION REPORT NUMBER

9. SPONSORING / MONITORING AGENCY NAME(S) AND ADDRESS(ES)

U.S. Army Research Office
P.O. Box 12211
Research Triangle Park, NC 27709-2211

10. SPONSORING / MONITORING AGENCY REPORT NUMBER

ARO 32445.1-EL-ISP

11. SUPPLEMENTARY NOTES

The views, opinions and/or findings contained in this report are those of the author(s) and should not be construed as an official Department of the Army position, policy or decision, unless so designated by other documentation.

12a. DISTRIBUTION / AVAILABILITY STATEMENT

Approved for public release; distribution unlimited.

12 b. DISTRIBUTION CODE

13. ABSTRACT *(Maximum 200 words)*

Photoconductive semiconductor switches have unique advantages such as high power, speed, negligible time jitter and long lifetime. Silicon carbide (SiC), due to its high dielectric strength and other desired properties, is an excellent material for photoconductive switches. However, no appreciable result has been reported on cubic silicon carbide (3C-SiC) photoconductive switches. In this research, photoconductive switches were fabricated on the following three types of 3C-SiC substrates: (i) boron doped, (ii) unintentionally doped single crystals and (iii) polycrystalline 3C-SiC. The switches were investigated using ArF and XeCl excimer lasers. Practical switches with many potential applications were successfully fabricated. The best results were obtained from the switches made from the polycrystalline material. The dark resistivity of the material was about 10^6 Ω cm. The operating breakdown field was 2.5 x 10^5 V/cm, which is the highest reported for all lateral geometry photoconductive switches, and was limited by the surface flashover effects. The highest peak photocurrent density through the switches was about 10 kA/cm^2. The ratio of the off-state resistance to the on-state resistance (R_{off}/R_{on}) was ~10^5, and the lowest on-state resistance was 45 Ω. The width of the photocurrent pulse was 15 to 30 ns which was limited by the laser pulse, indicating that the switches can operate in the megahertz range.

14. SUBJECT TERMS

SiC Polycrystalline

15. NUMBER IF PAGES

16. PRICE CODE

17. SECURITY CLASSIFICATION OR REPORT	18. SECURITY CLASSIFICATION OF THIS PAGE	19. SECURITY CLASSIFICATION OF ABSTRACT	20. LIMITATION OF ABSTRACT
UNCLASSIFIED	UNCLASSIFIED	UNCLASSIFIED	UL

DISCLAIMER NOTICE

THIS DOCUMENT IS BEST QUALITY AVAILABLE. THE COPY FURNISHED TO DTIC CONTAINED A SIGNIFICANT NUMBER OF PAGES WHICH DO NOT REPRODUCE LEGIBLY.

TABLE OF CONTENTS

LIST OF TABLES

LIST OF FIGURES

CHAPTER I

INTRODUCTION

A continuing theme in the development of pulsed electrical systems is the search for better switches. "Better" can mean: higher voltage, higher current, more efficient, faster turn-on, faster turn-off, fast recovery for higher repetition rates, easier control, more precise timing control for multiple switch systems, longer device lifetime, more reproducible operation, simpler, smaller, lighter, and less expensive. No conventional switch can satisfy all these requirements. However, photoconductive semiconductor switches, based on their unique characteristics, have the potential to fulfill virtually all of these requirements.

Since first demonstrated by Auston in 1975[1], photoconductors as high-speed electronic switches have drawn tremendous attention[2-7], because they have many advantages over conventional switches such as gas and mechanical switches. The advantages include: very fast switching, large dynamic range, scalability, negligible time-jitter response, high reliability, low inductance, simple mechanical structure, optical isolation of the trigger, high thermal capacity, immunity of noise, and flexible geometry allowing fabrication of low inductance structures.

1.1 ADVANTAGES OF PHOTOCONDUCTIVE SEMICONDUCTOR SWITCHES

1.1.1 Speed

High speed is one of the most important advantages of photoconductive semiconductor switches as power switching devices. Conventional pulsed power switches such as gas spark gaps and thyratrons, can operate only at frequencies as high as a few kilohertz and typically run much slower. In contrast, photoconductive semiconductor switches, being controlled optically, turn on and off much faster than is possible with any

other switching mechanism. They can operate as toggling switches at high frequencies above the megahertz range. Some of these switches made from direct transition semiconductor materials, for example, gallium arsenide, can operate at frequencies even higher than 10 GHz[8-10]. The high speed is determined by the extremely short rise time and fall time of photoresponse pulses of the switches. The rise time of the pulses, or the turn-on time, is from several nanoseconds to several picoseconds, and so is the fall time, or turn-of time. As a result, the switching time of photoconductive semiconductor switches can be controlled very precisely. They can be turned on and off with an accuracy up to several picoseconds.

With this timing accuracy of switching, photoconductive semiconductor switches can control large pulsed systems with negligible time-jitter. In many applications, a single switch cannot meet the operation requirements. For example, the applied voltage or the current to be switched is too high. The remedy for that is to connect a number of switches in series or in parallel. However, a time-jitter problem will come with this solution for most of the conventional switches because of their low speed. Photoconductive semiconductor switches, however, do not have this problem. Since their turn-on and turn-off time is only a few picoseconds, the time-jitter for each single switch is negligible for many applications. Further, since the switches are optically controlled, switches at different positions in a system can be activated simultaneously. This property together with the timing accuracy of photoconductive switches makes the pulsed power systems nearly time-jitter free.

1.1.2 Large Dynamic Power Range

Photoconductive semiconductor switches have a large dynamic power range. They can be used to switch small signals for testing and calibration, and can also be used for driving optoelectronic devices such as Pockell's cell[11-13], due to their excellent control of turn-off and turn-on or the high off-state resistance and sensitivity to the excitation light source. More importantly, they can also be used in super power systems[14-17]. This is

because these switches can withstand high voltage and handle large current. Since the switch resistance changes many orders of magnitude before and after being illuminated, the switches biased at high voltage can switch huge current. Semiconductor materials have very high dielectric strength. Typically their breakdown electric fields vary between 10^5 to 10^7 V/cm depending on the materials. A switch with one centimeter electrode separation can hold off 100 kV to 10 MV. Photoconductive semiconductor switches also have large current handling capability. The peak current density which can flow through switches depends on the power of the excitation light source. The maximum current density is determined by the maximum carrier density of the material and the rate the heat is removed. Semiconductor materials have the potential to create carrier densities of 10^{17} - 10^{20} cm^{-3}. It has been demonstrated that the electron-hole plasma densities in excess of 10^{17} cm^{-3} can be generated in semiconductors by the absorption of single picosecond optical pulses[18]. There are many optical sources which have enough power to reach this potential free carrier density, an excimer laser is a good example. Semiconductor materials have high thermal conductivity (compared to gas spark gap and other switches) and hence fast heat removal. This allows the switches to handle high power. It has been demonstrated that photoconductor semiconductor switches can switch pulsed power at gigawatt levels[19, 20].

1.1.3 Scalability

Scalability in terms of voltage, current, heat removal, and inductance is another feature of photoconductive semiconductor switches. As needed, the parameters of the devices such as maximum power, current and voltage handling capability, can be set by changing the size of the switches, because switch hold-off voltage scales with switch length, and current handling ability scales with switch width and thickness. Thus, the switches can be scaled from very small dimensions to very large dimensions without sacrificing the precise, high-speed control. Since the rate at which the photoconductive

effect produces electrons and holes in semiconductor materials is dependant only on the power of the optical source, for a given optical energy deposited on the switch surface, the on-state resistance is independent of switch width. Thus, the width can be increased when necessary without changing the switch performance. Widening the switch for a selected length results in several major advantages: the joule heating per unit width , the current per unit width, the optical energy density on the material, and the total device inductance are all decreased. Thus the average power and the peak power of the switch scale with the switch width.

1.1.4 Immunity from Noise

Finally, photoconductive semiconductor switches have excellent immunity from noise. The switches use lasers as their optical sources to control turn-on and turn-off. The optical energy of the laser must be higher than the bandgap of the semiconductor materials to turn the switch on. Thus, the noises, such as light and other electric magnetic radiation, whose energy is less than the bandgap, cannot affect the switches. The switches made from wide band gap materials such as SiC have larger noise immunity. Also because the switches are optically controlled, the controlling systems can be isolated from the power systems. In addition to that, because lasers propagate in well controlled directions, the switches can be designed in such a way that only the laser source can reach them while the noises can not.

These advantages of photoconductive semiconductor switches together with their performance reliability, structural simplicity, and long lifetime potential make them perfect choices for many pulsed power systems, especially in relatively large facilities that need particularly high performance switches not otherwise available. Many applications have been developed. Currently, the quality of conventional semiconductor materials, such as silicon and gallium arsenide, has improved and many new materials with high dielectric strength and other desirable properties for photoconductive semiconductor switches, such

as silicon carbide, are being developed. Light sources with large pulsed power are also available. Therefore, many more applications can be envisioned.

1.2 APPLICATIONS

Applications of photoconductive switches involve high-speed detectors for communication and diagnostics, synchronization of the outputs of multiple impulse generators, high-voltage short pulse generation , high-power ultra-wide band microwave generation comparable to those produced by thermonuclear explosions, optical pulse shaping and production of high-contrast pulses[21], picosecond spectroscopy and millimeter-resolution optical ranging, and so on. Some of these applications include compact high-voltage subnanosecond pulsers, high current particle accelerators, optically activated electrical firing sets (explosive detonators), ultra-wide bandwidth radar, super high energy storage systems, laser fusion systems, which need accurately synchronized high-voltage electric pulses, and flash x-ray power supplies. The following examples show the importance of photoconductive semiconductor switches in pulsed power systems.

1.2.1 Superpower Generator

Most superpower generators are multimodular because there are practical limits to the power one can extract from a single module. Further, it is less risky and expensive to create a working module and then to multiply that proven unit than it is to create a single, full-power module. A critical point is that having decided on a module design, one must synchronize the modules. For the superpower pulser case, the synchronization must be at the nanosecond level. Synchronization of conventional switches such as spark-gap switches is a limitation on superpower generator design and operation because of their low speed. Two factors combine to limit the ability of these switches to create short high-peak power pulses. Clearly, the pulse length can be no shorter than the sum of the rise and fall times, and the peak power will be of the order of the output energy divided by this time.

The pulse time is limited in two ways. The first is the shape of a single module's output pulse, and the second is the ability to synchronize the modules. Photoconductive semiconductor switches, owing to their high speed and precise time-control, can bypass these problems. Since the rise and fall time of their photoresponse pulse can be as short as picoseconds, synchronization at nanosecond level is no longer a problem. Also, since the pulses are much shorter than that of conventional switches, much higher peak power can be reached.

1.2.2 Inductive Energy Storage Pulsed Power System

Figure 1.1 shows the capacitative energy storage pulsed power system. Energy is stored in the electric field between the capacitor plates. When the switch is closed the

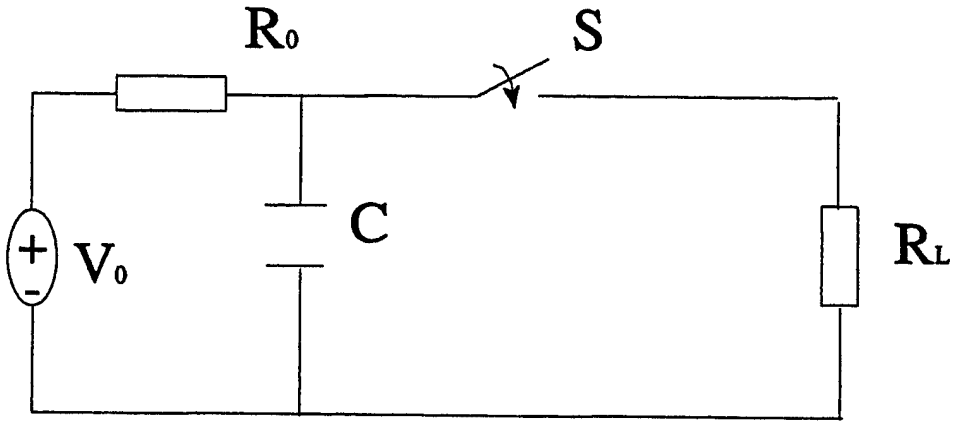

Fig. 1.1: Capacitive energy storage pulse system

capacitor discharges, delivering its energy to the load, R_L. Unfortunately, high-voltage, high-value capacitors are usually very bulky and quite inconvenient for many pulsed power applications. This problem can be avoided by using inductive energy storage pulsed power systems, where energy is stored magnetically rather than electrically. Figure 1.2 is the basic circuit. When the switch is closed, the inductor is charged to the current $I_o = V_o/R_c$. When the switch is opened the stored current is delivered to the load producing a

voltage pulse of peak amplitude,

$$V_{out} = I_o R_L = (R_L / R_C)\, V_o \qquad (1.2.1)$$

Thus, a voltage gain may be achieved if $R_l > R_c$. Nevertheless, high gain can not be achieved unless the following criteria are met: extremely fast switch opening (10 ns), on-resistance much lower and off-resistance much higher than the load resistance. Conventional switches such as plasma opening switches can not meet all of the criteria. Only photoconductive semiconductor switches can meet all the criteria simultaneously by choosing the proper material and excitation optical source. These switches can be opened in

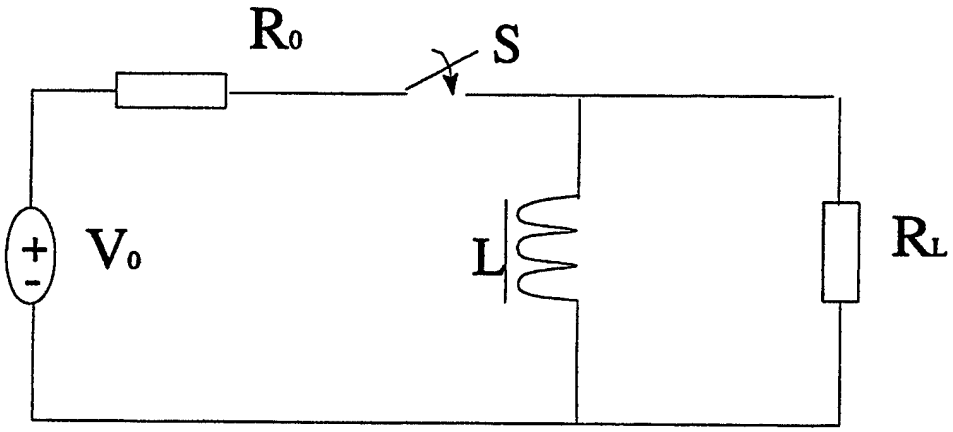

Fig. 1.2: Inductive energy storage power system

picoseconds, and their resistance changes dramatically controlled by optical source.

These examples illustrate only a few of the numerous applications of photoconductive semiconductor switches where they excel all other switches. The applications one can envision are virtually limitless, certainly beyond anything that this section might hope to enumerate. Photoconductive semiconductor switches have been suggested as replacements for most conventional pulse switches in high power and high frequency systems including spark gaps, thyratrons, and saturable inductors.

1.3 WHY SILICON CARBIDE

An ideal photoconductive semiconductor switch should have the following properties:

1. High dark resistance, so that the current leakage is low.
2. High hold-off voltage, so that it can be made small to handle high voltage.
3. Fast turn-on and turn-off, so that the timing precision of the switch control is high.
4. Low on-state resistance, so that it dissipates low power.
5. High power handling capability, which requires the switch to have the potential to sustain high current and voltage, efficient heat removal.
6. High sensitivity to excitation light source, so that it can be turned on with low optical power.
7. Resistant to high temperature, radiation, and chemicals, so that it can be operated in a severe envirement.
8. High mechanical strength, so that it is easy to handle.
9. Noise immunity.
10. Long lifetime.

Currently, the most commonly used materials for photoconductive switches are silicon and gallium arsenide. Although switches with high speed and high power handling capability have been demonstrated, these switches are not able to meet all the above requirements. The performances of these switches are limited by the relatively low dielectric strength, low thermal conductivity, and other related properties of the materials. Silicon carbide (SiC) is superior to Si and GaAs in many aspects. Table 1.1 lists some relevant physical properties of cubic silicon carbide (3C-SiC).

First, the dielectric strength of 3C-SiC (2 - 6 x 10^6 V/cm) is about 10 times higher than those of Si and GaAs, so higher voltages can be applied for switches made from SiC material. Thus for a certain desired voltage, SiC semiconductor switches can be made more compact. Compact switches require less optical energy to be turned on, because this energy

scales with the square of the switch length as follow [22].

$$R_S = L^2 h\nu/(E_a q\mu), \tag{1.3.1}$$

where R_S is the on-state resistance of the switch, L is the separation between the electrodes, E_a is the total energy absorbed from the optical pulse, $h\nu$ is the photon energy, q is the charge of electron, and μ is mobility ($\mu_n + \mu_p$).

Table 1.1: Physical properties of 3C-SiC

Parameter	Typical Value
Bandgap	2.2 eV
Breakdown Field	2 - 6 x 10^6 V/cm
Thermal Conductivity	3.9 W/cm°K
Saturated Electron Drift Velocity	2.5 x 10^7 cm/s

Secondly, since 3C-SiC is a wide bandgap material (2.2 eV), its intrinsic carrier density is much less than that of Si and GaAs. Thus the switch made from SiC has higher dark resistivity, lower leakage current, and a better opening state. Therefore, the energy dissipated by the switch is lower, and the system controlled by this switch has higher efficiency.

The thermal conductivity of SiC (3.9 W/cm°K), which approaches that of copper, is also higher than that of Si (1.5 W/cm°K) and GaAs (0.54 /cm°K). This property of

SiC gives the switches more efficient heat removal and hence high power handling capability. Further, since SiC is a wide bandgap material, its Si-C bonding energy is high, and hence it is resistant to high temperature and radiation, and possess high mechanical strength and chemical stability. With these properties, SiC switches can operate at high temperatures and in harsh environments, and are easy to handle.

In addition, SiC is superior to silicon and gallium arsenide in the following aspects. Switches made from silicon and gallium arsenide has problems called thermal runaway effect[23, 24] and lock-on effects[25 - 26] when operated at high voltages. Thermal runaway effect is caused by the materials' low thermal conductivity and low energy bandgap. It occurs in photoconductors when a voltage is applied to the switch, and the rate of thermally excited carrier generation exceeds the rate of thermally excited carrier removal through recombination and sweepout. This process leads to additional current flow and additional resistive dissipation in the switch, which increases the switch temperature, which increases the rate of thermal carrier generation and thus produces a regenerative runaway into complete conduction. To prevent thermal runaway from causing premature conduction, the switches made from these materials have to be operated in a pulse bias mode. This way, the thermal energy deposited in the switch can be removed before the voltage is applied to the switch for the next pulse. The low-power thermal runaway limits the application of the switches made from Si and GaAs. For SiC, however, due to its high thermal conductivity and wide bandgap, it is very difficult to reach the temperature at which thermally excited carrier generation exceeds carrier recombination. Lock-on effect is a type of premature breakdown. Although Si and GaAs have nearly the same breakdown field which is about 200 kV/cm, the switches made from these materials can only work at much lower electric fields[27]. When the field exceeds 3.5 kV/cm, the switch does not turn off after being turned on by a light pulse[28,29]. In fact, it stays in the on-state as long as the voltage is applied. The mechanism of lock-on effect is not yet understood. This effect limits the switch hold-off voltage and speed.

With the above advantages and its high saturation drift velocity (~ 2 x 10^7 cm/s), silicon carbide is a very promising material for photoconductive semiconductor switches, especially for switches operating in a speed range between kilohertz and megahertz. Although the optoelectronic potential of SiC has been known since 1907[30], only recently has device-quality SiC material been available[31]. As a consequence, a lot of work needs to be done to exploit the application of this material for electronic devices. Initial results for hexagonal silicon carbide (6H-SiC) photoconductive semiconductor switches have been reported by S. Saddow , et al[32-33]. However, high dark resistance and high applied voltages have not been obtained. The photocurrent response is also relatively slow. These switches cannot be made into practical power switching devices. No data have been reported yet for 3C-SiC photoconductive semiconductor switches. Since 3C-SiC has a small lattice mismatch with silicon, it can be directly grown on a silicon substrate. For this reason, it is thought to be a potential low cost material. Fabricating photoconductive switches from 3C-SiC is economically and technologically important. Therefore, 3C-SiC photoconductive switch is a very promising power switching device.

CHAPTER II

THEORY

The basic photoconductive semiconductor switch is used to connect a power supply to a load and consists of two electrical contacts separated by a highly resistive semiconductor material, normally semi-insulating or intrinsic semiconductor material as shown in Figure 2.1. Since its dark resistance, or off-state resistance, is very high, it is

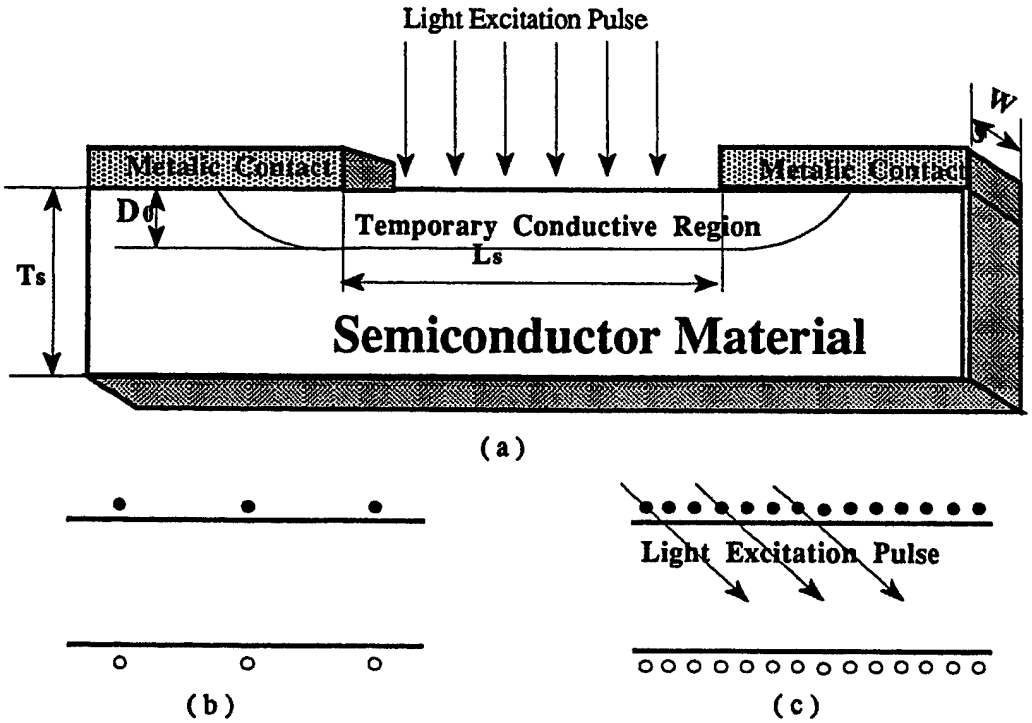

Fig. 2.1: (a) Structure of photoconductive semiconductor switch, and band diagram.. (b) Before excitation, the carrier density is low. (c) After excitation, excess electron-hole pairs are created.

considered as normally open and no current flows through the switch. To close the switch, the region between the contacts is excited with a proper light source, which is absorbed by the photoconductive material, producing free carriers (electron-hole pairs) as shown in Figure 2.1c. The resistance dramatically decreases, so the excitation produces highly conductive path between the electrodes. Thus the switch starts to deliver power from

source to the load. After the light pulse ends, the generated electron-hole pairs recombine very quickly. As a result, the semiconductor material returns to highly resistive state from a highly conductive state, and the switch opens again, stopping delivering power from the power supply to the load. The thickness of the semiconductor slab, D_S, should be larger than the optical absorption depth, D_0, so that all of the optical energy of the light source is used to turn on the switch. The switch resistance is controlled by uniform optical illumination between the contacts as indicated by the optical pattern shown in Figure 2.1. The length of the switch or the distance between the electrical contacts, L_S, or electrodes is determined by the required operating voltage. The width of the semiconductor slab, W_S, should be determined by the desired system inductance, the required current handling capability, and the desired thermal resistance from the switch to the surrounding medium.

2.1 OFF-STATE RESISTANCE

The "open" or off-state resistance, R_{off}, is determined by the dark or steady-state resistivity of the semiconductor slab, p_0, or

$$R_{off} = p_0 L_S / (W_S D_S). \tag{2.1.1}$$

The resistivity is determined by the standard resistivity equation

$$p_0 = 1/[(ne\mu_e) + (pe\mu_h)], \tag{2.1.2}$$

where n and p are the electron and the hole density, respectively, e is the electron charge, and μ_e and μ_h are the electron and the hole mobilities, respectively. As mentioned above, the off-state resistance should be as high as possible. Thus the electron and hole density

should be as low as possible. This naturally leads to the requirement that the semiconductor material is intrinsic or compensated. An effective method of increasing the dark resistivity is to introduce a moderate density of deep level defects into the semiconductor which act as traps. This can be done by ion bombardment[34, 35], radiation damage[36], and use of materials with large naturally occurring defects such as polycrystalline and amorphous semiconductors.

The dark resistivity is important from the system design point of view because the dark resistance determines the value of the leakage current flowing through the switch before it is turned on. The preswitching current through the semiconductor switch dissipates energy in the switch, which causes an off-state heating problem. Further more, this current flows through the whole system and dissipates energy in the load. This may effect the function of the entire.

2.2 ON-STATE RESISTANCE

The resistance of a photoconductive semiconductor switch decreases when optical control energy is applied to the surface of the switch. The on-state resistance depends on the power and the wavelength of the optical source. Assuming the switch surface is uniformly illuminated between the electrical contacts, the equations (2.1) and (2.2) can be used for the on-state resistance. In this case, n and p are the generated, excess carrier densities, which are much higher than dark carrier densities. Incident photons create electron-hole pairs, such that, $n = p$, thus the on-state resistivity can be written in terms of an effective mobility, μ, which is the sum of the electron and hole mobilities,

$$\rho_0 = 1/ne(\mu_e + \mu_h) \equiv 1/ne\mu. \qquad (2.2.1)$$

The on-state resistance can now be written as

$$R_{on} = p_0 L_S / W_S D_S = (1/ne\mu)(L_S / W_S D_S), \qquad (2.2.2)$$

where D_S is the optical absorption depth of the excitation light source in the semiconductor material. The absorption depth is determined by the wavelength of the light . The shorter the wavelength, the smaller the absorption depth. In order to pump electrons from the valence band to the conduction band, the photon energy from the light source must be greater than the band-gap of the semiconductor material. The semiconductor-optical source couple is usually chosen such that the optical absorption depth is much less than the semiconductor thickness to insure that all the optical energy is absorbed. The absorption depth of the excitation optical source in the switch should not generally exceed the skin depth for a particular application, because switch efficiency would be lost if the entire conducting volume were not used. The skin depth, d in the optically controlled switch is given by[37]

$$d = (\pi f \mu_0 s)^{-0.5} = (\pi f \mu_0 ne\mu)^{-0.5}, \qquad (2.2.3)$$

where f is the operation frequency of the circuit, μ_0 is the permeability of free space, and σ is the electrical conductivity of the material. If every photon of the optical source creates a electron-hole pair, then n is equal to the number of the photons.

2.3 MAXIMUM DARK HOLD-OFF VOLTAGE

Dark hold-off voltage is the voltage the photoconductive semiconductor switch can withstand (hold-off) before being optically turned on. The maximum hold-off voltage of the switch is determined by material's dielectric strength or the maximum breakdown

electric field, the properties of the contact metals, the shape of the electrodes, the surrounding media of the switch and the length of the switch. A large breakdown field is required to obtain a high dark hold-off voltage. In many designs, the electric breakdown strength of an interface between two materials is usually significantly lower than the bulk electrical breakdown strength of the material. This is caused by the surface dielectric strength failure or surface flashover[7]. At the points of contact between the semiconductor surface and the metal electrodes, the combination of different material properties and high electric fields can produce free electrons. Free electrons in a high electric field region serve to seed surface charge multiplication and surface electric field enhancement. One method to increase the surface dielectric strength is to place the contacts in a low electric field region by specifically designing the surrounding geometry[38]. Immersing the switch in media with high dielectric strength, including gas and liquid, can also ease the surface flashover effect[39].

Since the dielectric strength of the photoconductive semiconductor switch is a constant, its maximum dark hold-off voltage is proportional to the switch length. Increasing the distance between the electrodes can increase the hold-off voltage. However, the optical energy required to change the switch resistance scales as the square of the length of the switch. Thus it is desirable to use the minimum switch length for the maximum electric field. This once again shows the importance of high dielectric strength materials for photoconductive semiconductor switches.

2.4 POWER HANDLING CAPABILITY

The practical maximum current that can be conducted through a photoconductive semiconductor switch is determined by the physical effects dependant upon the carrier density. The maximum carrier density, n_{max}, is related to the maximum current density, J_{max}, by

$$J_{max} = n_{max} e v_d = n_{max} e \mu E \qquad (2.4.1)$$

where v_d is the carrier drift velocity, e is the charge of an electron, μ is the sum of the electron and hole mobilities and E is the conduction electric field in the switch. Therefore, the maximum carrier density determines the optimum peak current density that can flow through the switch. The maximum carrier density in silicon has been determined to be on the order of 5×10^{17} cm^{-3} by investigating the relative carrier density effects related to Auger recombination, free carrier absorption, and the slope of the thermal conductivity as a function of carrier density[40]. This carrier density corresponds to a peak current density in silicon of approximately 60 kA/cm^2. On the other hand, the current through the switch creates heat, causing temperature increase. When the temperature increases to a critical point the switch stops performing properly. Thus the power handling capability is also determined by the rate of heat removal. If the material has high thermal conductivity and thermal stability, then the switch can handle large power. SiC, for example, possesses the required properties.

2.5 SWITCHING SPEED

The speed of photoconductive semiconductor switches depends on the excitation light source as well as the carrier lifetime in the semiconductor materials. The switch turn-on and turn-off speeds are determined by the rise and fall times of the photocurrent. The rise time of photocurrent is usually the same as that of the light pulse because the light sources used for the switches have very short rise time (picoseconds to several nanoseconds), and the electron transition from valence band to conduction band virtually takes no time. The fall time is determined by both the fall time of the light pulse and the

carrier recombination time. When the recombination time is short relative to the light pulse duration, the photocurrent pulse will roughly follow the light pulse profile. When the recombination time is long, it is equal to the fall time of the photocurrent pulse. Recombinations occur through both bulk and surface effects. The recombination in the bulk can be divided into three types[41]: band-to-band recombinations, impurity and defect recombinations, and Auger recombinations. Band-to-band recombination, which includes radiative recombinations, is slow in indirect bandgap materials but fast in direct bandgap materials. Auger recombination involves a collision of three particles, *i.e.*, two electrons and a hole, or two holes and an electron. The three-particle character of Auger transitions gives rise to a recombination rate which is proportional to the cube of the excess carrier density[42]. At high carrier densities, Auger recombination dominates. Impurities and defects act as very efficient recombination centers, which also speed up the recombination. The recombination is faster at the surface than in the bulk of a semiconductor, because of the surface states and because there are more defects and dislocations at the surface.

Introduction of defects into the semiconductors can reduce the free-carrier lifetime and increase the switch speed. The defects act as traps and recombination centers. As discussed earlier, this can be done by ion implantation, and use of materials with large naturally occurring defects such as polycrystalline and amorphous semiconductors. The capture time τ_c can be estimated from the expression[43]

$$\tau_c = 1/N_t \sigma_c \langle \upsilon_{th} \rangle, \qquad (2.5.1)$$

where N_t is the trap density, σ_c the capture cross section, and $\langle \upsilon_{th} \rangle$ the mean thermal velocity. Another advantage of high defect densities is an enhanced optical absorption in the spectral region below the edge for direct transitions due to the introduction of new states

and the relaxation of selection rules for indirect transitions. This effect is more pronounced in indirect bandgap materials such as silicon carbide. The major disadvantage of the use of high defect densities to produce short free carrier lifetime is the substantial reduction in carrier mobilities and in switch sensitivity due to increased elastic scattering from the defects. Estimates of the influence of elastic scattering on carrier mobilities from neutral defects are given by[44]

$$\mu = \frac{1.4 \times 10^{22}}{N_t} \frac{m^*}{m_o} \frac{\varepsilon}{\varepsilon_o} \qquad (cm^2/V.s) \qquad (2.5.2)$$

where m and m* are the mass and effective mass of electron respectively, ε and ε_0 are the dielectric constants of the material and vacuum respectively.

CHAPTER III

EXPERIMENT

3.1 MATERIALS AND SWITCH PATTERNS

Three following types of 3C-SIC materials were used to fabricated photoconductive semiconductor switches: (I) unintentionally doped single crystal material, (ii) boron doped single crystal material and (iii) polycrystalline material. Unintentionally doped SiC single crystal material was used first. The material was grown on silicon substrates using the chemical vapor deposition (CVD) method. The thickness varied between 2 μm and 10 μm. Although the quality of samples was good enough for fabrication of other types of device[45, 46], they did not meet the particular requirements for photoconductive semiconductor switch. The switch requires highly resistive materials, unfortunately the resistivity of the unintentionally doped samples was only about 100 Ωcm, which was too low. For this reason, these samples could not be used to fabricate practical photoconductive switches. In order to increase the resistivity, the materials was doped with boron during growth. Since boron is a deep level dopant in 3C-SIC, the atoms can remove the free carriers from the conduction and valence bands. The thickness of the boron doped samples was about the same as the unintentionally doped samples. Because the trapped carriers are difficult to activate thermally, the resistivity of boron doped 3C-SIC was expected to be higher than that of unintentionally doped SiC. The resistivity did increase, but only slightly. These samples also could not be used to fabricate practical photoconductive switches. Furthermore, the crystalline quality of the samples was lower than that of the unintentionally doped material.

Finally, polycrystalline 3C-SiC material was used for switch fabrication. This material was grown on a graphite substrate using the CVD method[48]. The graphite substrate was burned off after growth. The thickness of the samples was approximately 600 μm, which is desirable for power switching devices. Figure 3.1 shows a TEM

micrograph of the structure of the material. It can be seen that the material consists of crystalline grains. The average size of the grains is about 1.5 μm. The material is highly resistive and its dark resistivity is about 1 MΩcm. This value is virtually ideal for photoconductive semiconductor switches.

Fig. 3.1: A TEM micrograph of the polycrystalline structure of the poly 3C-SIC material.

The photoconductive semiconductor switches were fabricated as lateral geometry. There are several advantages gained by using a lateral geometry switch. It is faster than a vertical switch because the surface states of the material contribute to speed up the free carrier recombination. It is scalable, *i.e.*, its power handling capability scales with its size. The structure of a lateral switch is simpler than a vertical switch. It is more efficient because the light source shines directly into the semiconductor material, which is not the case for vertical switch. For a vertical switch, the light has to pass the transparent electrode first before penetrating into the semiconductor, thus part of the light is absorbed by the electrodes. Most of the switches were fabricated into interdigitated patterns as shown in Figure 3.2. This way, high current can be delivered by a small switch. Since the optical power required to turn on a switch scales with the square of the length of the switch gap, a small switch requires less power than a large switch. Three switch gap spacings 2, 5 and

10 μm were made. The width of the "fingers" is 10 μm, the distance between the pads is 800 μm, and the area of the pads are 800 x 240 μm^2. In order to reach a high hold-off voltage, single strip gap switches were also fabricated so that higher voltages could be applied. The gap spacing for these switches ranged from 40 μm to 200 μm.

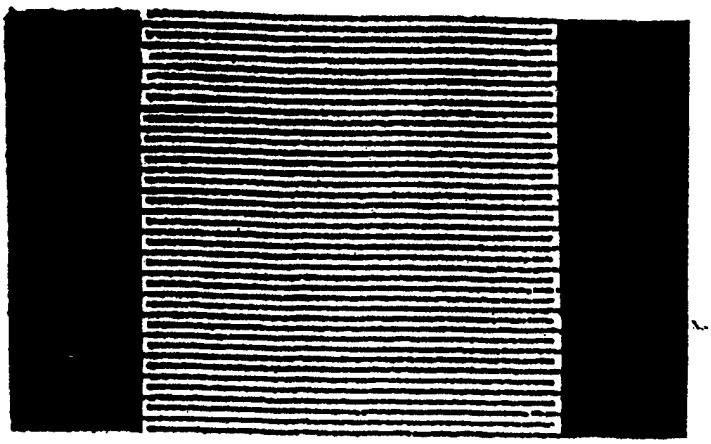

Fig. 3.2: The interdigitated pattern of the photoconductive semiconductor switches

3.2 PROCESS AND FABRICATION

3.2.1. Process for Polycrystalline 3C-SIC Substrate

Since the polycrystalline 3C-SIC samples were thick, they are easy to handle. Standard process procedures were used in the switch fabrication. The fabrication process includes the following steps:

A. Sample preparation

Standard cleaning procedures were applied to the samples, which include the use of DI water, soap, camel brush, cotton q-tip, T.C.E., acetone, methanol, NH_2OH, H_2O_2, ultrasound, and so on. Due to the requirement of high hold-off voltage for the switch, the surfaces must be very clean in order to reduce the surface flashover effect. Dust and surface imperfections, which localize the electric field across the switch, can easily cause premature surface breakdown. In order to avoid this, the surfaces were also carefully polished and cleaned with a buffered HF solution.

B. Photolithography

Two types of photoresists were used: SPR 505L-A and Shipley S1808. Their thicknesses were approximately 0.46 μm and 0.8 μm respectively after spinning at a speed of 4000 rpm for 30 seconds. The developer was Microposit 351, and the develop time was between 8 and 25 seconds, depending on the thickness of the photoresist. Two mask-aligners, the Karlsuss MJB3 Deep UV Mask-aligners and PLP UV Maskaligner, were used for alignment and exposure. The two aligners used a 250 nm Hg/Xe Short Arc lamp and a 345 nm mercury lamp, respectively. Exposure times were chosen to be about 10 seconds for both aligners. The photomasks used with the PLP UV maskaligner were made of sodalime, while the photomasks used with the Karlsuss system were made of quartz because sodalime absorbs deep UV light. One difficulty was encountered in the device fabrication. During lift-off the photoresist was not completely removed, and as a result, some device patterns did not come out clearly. This is because that the resists were not thick enough. To overcome this problem, bilayer photoresists were used. First, S1808 was coated on the samples, and baked at prebake temperature (95 °C) for 5 minutes. SPR 505L-A was then coated on the top of the S1808, and the samples were then baked at the same temperature for 20 minutes. After using this bilayer coating of photoresist, liftoff was no longer a problem.

C. Ohmic Contact

Ohmic contacts were made by evaporating metals onto the samples using electron beam evaporator followed by stripping and Rapid Thermal Annealing (RTA). Different metals including Al, Ni-Au, Ti-Al, Cr-Mo-Au were used to make the electrodes of the switches. There were two purposes for using different contact metalization. One purpose is to find a good ohmic contact system for the switches. The other purpose, which was more important, was to find a contact metalization system such that the surface flashover effect could be reduced, or higher applied voltage could be sustained by the photoconductive switches. In that sense, ohmic contact is not very important. Because at high voltage, the

contact barrier breaks down. Photoconductive semiconductor switches operating at high voltage are virtually junctionless devices.

When Al was used as an ohmic contact metal, a simpler and more efficient method than the bilayer photoresist method was also used to overcome the liftoff problem. In this new method, Al was evaporated after the samples were cleaned. Photolithography was then done using positive instead of negative photomasks. After developing, the photoresist pattern was negative. In other words, the undesired metal area was exposed and the desired area was covered by the resist. The samples were then placed in a $H_3PO_4/CH_3COOH/H_2O$ (90 : 19 : 5) solution to etch away the exposed area. The unetched metal, which was covered by photoresist, formed the electrodes of the switch. The switches patterns made this way was clearer than those made the bilayer method.

D. Wire Bonding

Gold wires with a diameter of 40 μm was used and were bonded to the samples by silver glue. This step was performed by hands under a microscope. The wires were carefully attached to the samples at the switch electrode pads. The samples were then baked at 170 °C for 30 minutes to secure the bonds.

3.2. FABRICATION PROCESS FOR SINGLE CRYSTAL 3C-SIC FILMS

As mentioned earlier, the unintentionally doped and boron doped samples were grown on silicon substrates, and their thickness ranged from 2 to 10 μm. Because the SiC films were thin, the excitation light might pass through them and penetrate into the silicon substrates, and generate free carriers which would create a photocurrent in the substrate. This photocurrent signal would in turn mix with the current created in the SiC film, so that the correct photoresponse of the SiC could not be measured. In order to eliminate this effect, the substrate was etched away after the ohmic contacts were made. However, because the film was very delicate, special care was taken. First, the sample was put on a hot plate, and was attached to a piece of sapphire using wax with the device patterns facing

it. The devices were protected. The silicon substrate is then etched away in buffered HF/HNO_3 solution. The remaining thin SiC layer was then flipped over onto a piece of glass with a piece of thermal plastic between them. By heating up the sample on the hot plate, the plastic melted and the sapphire was taken away. When the sample cooled down, it was attached to the glass piece by the thermal plastic. Thus the side with device patterns finally was exposed, and wire bonding could be done. After this treatment, the thin film could be easily handled.

3.3 EXPERIMENT SETUP

Figure 3.3 is the block diagram which represents the experimental setup used to investigate the performances of the photoconductive switches. The switch was activated by an excimer laser. The photocurrent pulses were detected with help of an oscilloscope.

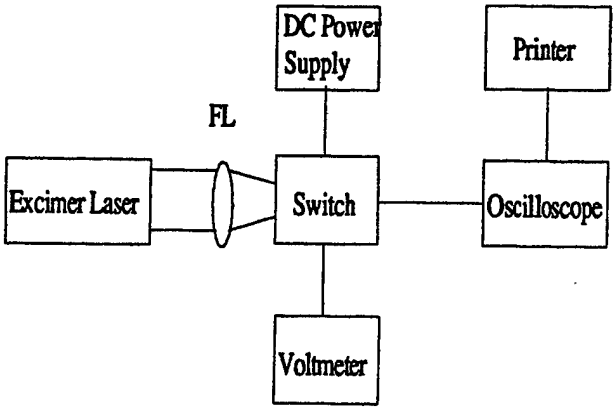

Fig. 3.3: Eperimental setup for testing the photoconductive semiconductor switches

Excimer lasers were chosen because they have high output powers and short pulses. The two lasers used were argon fluoride (ArF) and xenon chloride (XeCl) excimer lasers. Table 3.1 gives the operating parameters of these lasers. As can be seen from this table, the photon energies of both lasers are lager than the bandgap of 3C-SIC (2.2 eV). Thus these lasers can pump electrons from the valence band to the conduction band, which in turn

Table 3.1: Operating Parameters of ArF and XeCl Excimer Lasers

Laser Type	Wavelength (nm)	Photon energy (eV)	Pulse Width (ns)	Pulse Energy (mJ)	Frequency (Hz)
ArF	193	6.4	15 - 20	30 - 50	1 - 200
XeCl	308	4.1	75	90 - 140	1 - 200

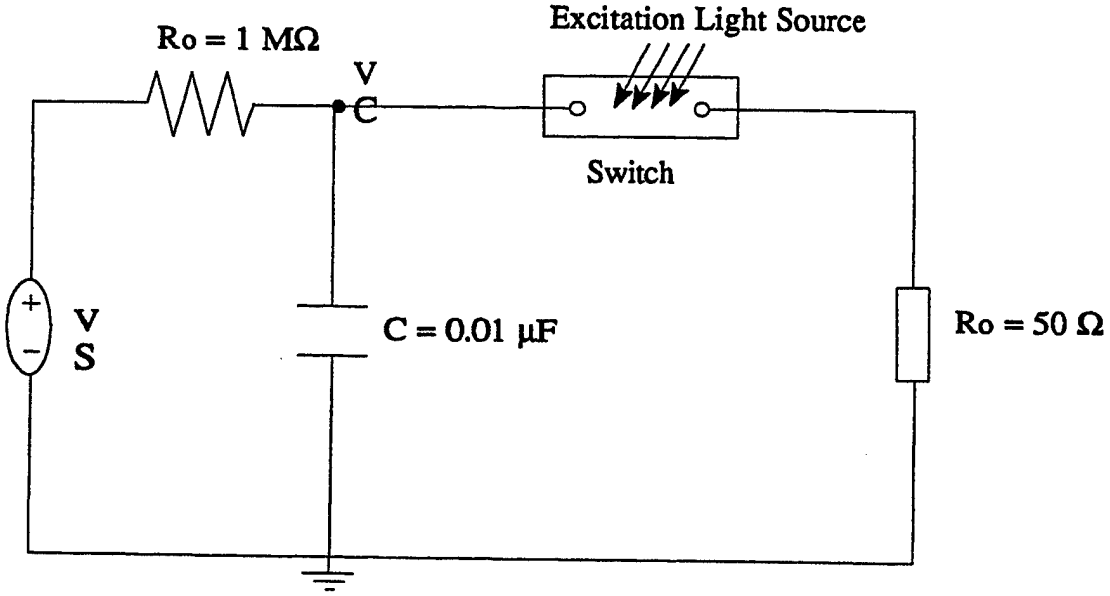

Fig. 3.4: Photoconductive Semiconductor Switch Test Circuit

changes the material from resistive to conductive. The ArF excimer laser was used at early stage of the investigation, but because of its small wavelength, its absorption depth in 3C-SiC was less than 1 μm[49, 50], and only very thin layer of the SiC was activated. In order to increase the absorption depth, the gas of the excimer laser was changed from ArF to XeCl in the later stage of this experiment. The wavelength of the XeCl laser is 308 nm and its absorption depth in 3C-SIC material is greater than 1 μm[49,50]. Figure 3.4 shows the output laser pulse temporal profile of the XeCl laser.

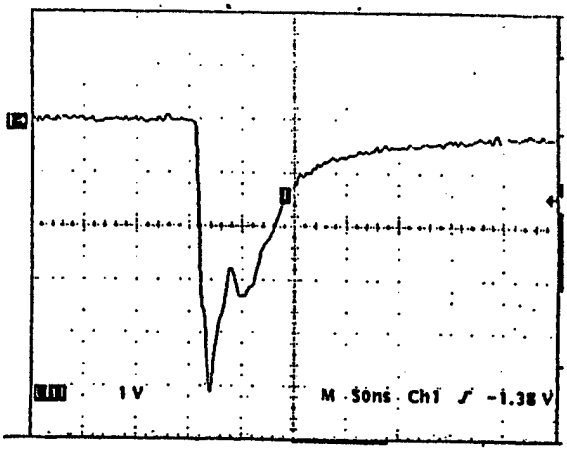

Fig. 3.5: Output pulse temporal profile of XeCl excimer laser

The switch block consisted of a photoconductive switch and a test circuit, which were mounted in a small metal box. The box had a window for the excitation laser, and the circuit was connected to the outside with screened cables. This way, the photoresponse signal was protected from the electromagnetic radiation from various sources. The circuit is shown in Figure 3.5. The DC power supply used was a Varian High Voltage Power Supply, MODEL 3000R, which had a current limit of 1 mA. The resistor R_0 (1MΩ) was used to protect the power supply, because when the switch is activated, its resistance became very small, and without R_0, the current through the power supply would have been very high and would have damaged it. With R_0, the current was limited. The purpose of capacitor C (0.01 μF) was to store the energy to be delivered to the load, and keep the voltage V_C unchanged when the switch is optically activated. Again, due to the low on-state resistance of the switch, the voltage V_C would have been very low without the capacitor, so that only very small power could have been switched. With this capacitor, the value of V_C remains almost the same before and after the switch is activated, or is independent of the switch resistance. Thus, high power can be switched. The capacitor was chosen to meet the following requirements, $R_L.C >> \tau$, where τ is the pulse width of the photocurrent,

and it can sustain high voltage, up to 1000 V.

The load or the 50 Ω resistor is the oscilloscope input impedance. The oscilloscopes used to monitor the photoresponse pulse were the Tektronix TDS320 Digitizing Oscilloscope and the HP-54502 Digitizing Oscilloscope, with sampling rates of up to 100 MHZ and 400 MHZ, respectively. Waveforms can be stored in the oscilloscopes and be sent to a printer. The voltmeter was used to monitor the voltage V_C while changing the power supply voltage, V_S. By knowing V_C and V_S, we can find the dark resistance of the switch.

3.4 SWITCH INVESTIGATION

The switch performances were investigated in the following aspects:

1. The dependence of the peak photocurrent, the on-state resistance, and off-state resistance on the bias applied on the switches.

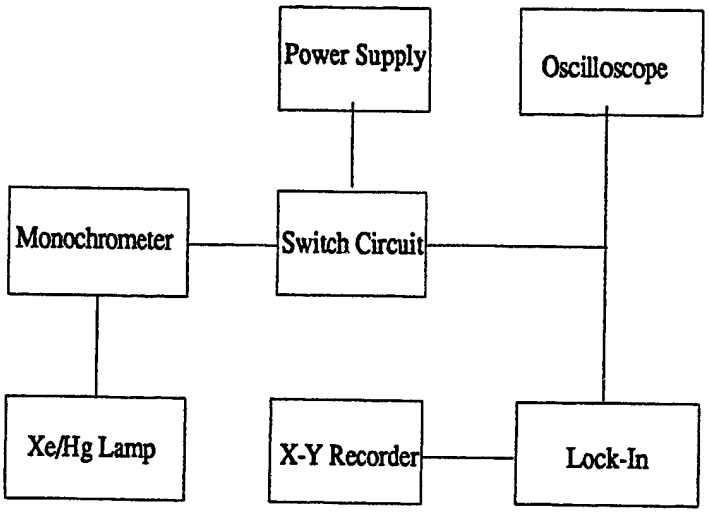

Fig. 3.6: Block diagram used to measure the spectrum of the switches

2. The dependence of the photocurrent, the on-state resistance, and off-state resistance on the excitation light power density. This was done by changing the distance between the

switch and the focus lens (FL) as shown in Figure 3.2.

3. The dependance of the photocurrent, the on-state resistance, and off-state resistance on temperature. We used the same circuit and placed the switches in a furnace. The temperature was controlled by a voltage transformer and monitored by a thermometer.

4. The switch breakdown voltage with different contact metals: Al, Ti/Al, Ni/Au, Cr/Mo/Au.

5. The switch breakdown voltage in the air and in a liquid called fluorinert. Fluorinert possesses high dielectric strength, which is 181 kV/cm at room temperature. This dielectric strength is higher than that of air. The purpose of using fluorinert was to suppress the surface flashover effect, so that higher switch breakdown voltage in the liquid was expected.

6. Comparison of the performances of the switches when activated with two different lasers, ArF and XeCl excimer lasers.

7. The switch photoresponse to the light from Xe/Hg lamp, and the photoresponse spectrum measuring. This measurement was made using the setup shown in Figure 3.6.

CHAPTER IV

RESULTS AND DISCUSSION

4.1 SWITCHES FABRICATED ON POLY 3C-SIC SAMPLES

4.1.1 Switch General Performances

A. Photocurrent, Off-State and On-State Resistance

Figure 4.1 shows the typical photocurrent pulse from a switch with 10 μm gap spacing when illuminated by ArF excimer laser. The pulse was measured on a 50 Ω resistor with a 5 times attenuation connected to the oscilloscope input terminator. The oscilloscope was operated in a DC mode. The DC bias on the switch was 100 V. The laser pulse energy was 50 mJ, and the pulse repetition rate was 10 Hz. From the Figure 4.1,

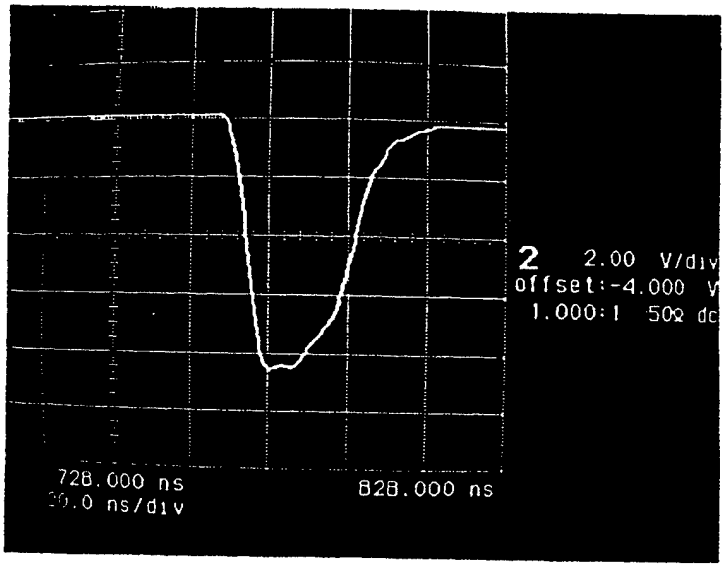

Fig. 4.1: Photocurrent pulse measured on 50 Ω resistor with a 5x attenuator. Bias on the switch is 100 V, laser pulse energy is 50 mJ.

we can not see any dark current or current leakage, indicating that the switch off-state resistance is ideal. The current leakage was only $I_{Dark} = 22$ μA. As can be seen, the pulse peak voltage of the pulse is about 8.6 x 5 = 43 V, corresponding to the peak photocurrent,

Ip = 0.86 A. With these data, it can be found that the switch on-state resistance was R_{on} = 66 Ω. Therefore, the ratio of the switch off-state resistance to the on-state resistance is 6.8 x 10^4, *i.e.* R_{off}/R_{on} = Ip/ I_{dark} = 6.8 x 10^4. This is only a typical example of the results we got from many our photoconductive switches. The lowest on-state resistance reached was about 45 Ω for 10 μm gap switches, the highest off-state to on-state resistance ratio was about 1.0 x 10^5. The highest peak photocurrent was

$$Ip = 1.7 \text{ A.} \tag{4.1.1}$$

According to articles [49, 50], we can assuming the absorption depth to be 0.5 μm, so that the corresponding current density was

$$Jp = 10 \text{ kA/cm}^2. \tag{4.1.2}$$

B. Hold-Off Voltage

The highest breakdown voltage reached was 250 V for 10 μm switches, the corresponding electric field was 250 kV/cm. This, to our knowledge, is the highest breakdown field ever reported for all lateral photoconductive semiconductor switches. However, it is still about one order of magnitude lower than the breakdown field of 3C-SIC. The switch breakdown happened on the switch surface, caused by surface flashover, see Chapter 2. The spark on the surface was observed when the breakdown occurred. The electrodes of the switch was damaged after breakdown. The following experiment also proved the surface flashover effect. When the metal contact was not annealed after evaporation, the breakdown voltage of the switch was much lower than that of the switch annealed.

Experiment showed that between the switches of a particular pattern made on

different samples or different spots of a given sample, there was significant variation in the performance. The hold-off voltage ranged from 150 to 250 V, and the peak photocurrent under same external conditions could change several times. This could be caused by the non-uniformity of the material's electronic properties. It could also have been introduced during the fabrication process.

C. Speed

As can be seen, the pulse full width at half maximum (FWHM) is about 24 ns, the full width about 50 ns, and the rise time about 10 ns, fall time about 30 ns. It was found that the widths of the current pulses for different switches were different. The FWHM ranged between 15 ns and 30 ns. The photocurrent pulses in Figure 4.2 and Figure 4.3 show the different pulse widths. This change of pulse width was probably caused by the test circuit. Unmatched impedance and parasitic capacitor in the circuit can widen the pulse waveform on the oscilloscope. It may also be caused by the change of experimental conditions in the fabrication process. A slight change in the condition may cause a major change in the switch capacitance and inductance. It may also be caused by the non-uniformity of the material. The shortest FWHM of the current pulse, 15 ns, is about the same as the pulse width of the ArF excimer laser pulse. Thus the speed of the switch response is limited by the laser pulse and the faster response could not be measured. We suspect the photoresponse of the 3C-SIC switches is faster than the limit of the laser pulse.

If we take 30 ns as the photoresponse pulse width, the switch can operate at a frequency 33 MHZ. This switching speed is much faster than that of conventional switches such as gas spark gaps and thyratrons (~ 1 kHz), and is also faster than that of silicon photoconductive switches (1 - 100 kHz)[7].

The 30 ns pulse width is much shorter than the carrier lifetime (~ 0.8 μs) reported for single crystal 3C-SIC materials[51]. This indicates that although SiC is an indirect band gap material and its carrier lifetime is relatively long, the defects and impurities in the

material can dramatically reduce the carrier lifetime. The defects act as traps and recombination centers[43]. As mentioned in Chapter 2, the carrier capture time τ_c can be

Fig. 4.2: The photocurrent pulse from a switch with 10 μm electrode gap. Bias = 80 V, vertical: 10 V/div, horizontal: 10 ns/div.

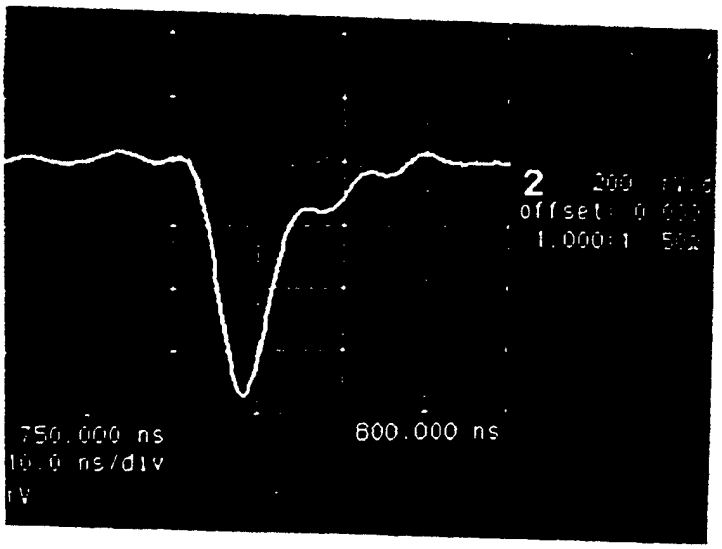

Fig. 4.3: The photocurrent pulse from a switch with 200 μm electrode gap. Bias = 50 V.

estimated from the expression $\tau_c = 1/N_t \sigma_c <\upsilon_{th}>$. In our poly SiC, since the density of defects N_t is very high so that the capture time τ_c is very short, which makes the carrier lifetime very short. The fast switching speed of the poly SiC witches experimentally proved the fact that the defects or impurities in indirect band gap materials can greatly decrease their carrier lifetime.

It was also noticeable that although the photocurrent pulse fells sharply approaching zero, it did not recover to zero completely for relatively long time. Similar phenomena was observed in small signal 6H-SiC switches by other researchers[52]. Correspondingly, while we monitor the switch resistance, we found that the switch resistance behaved the same way. When the laser pulse ended , the resistance increased very fast at first, but it took several seconds for the switch to recover to its dark resistance value. We believe this long tail is caused by the re-emission of carriers from the shallow traps that reside within the energy band gap[53]. This effect will be discussed again later in section (4.1.7).

Having known the peak photocurrent density and the critical point for the current saturation, we can estimate the carrier lifetime of the poly 3C-SIC. The laser spot size S is about 3.5 x 1.0 cm^2. Assuming a square laser pulse with pulse width of 30 ns and given the pulse energy of ArF laser, we can find the power density,

$$P_{laser} = 0.48 \text{ MW/cm}^2, \tag{4.1.3}$$

and the corresponding number of photons which hit the switch per square centimeter per second is

$$N_{ph} = 4.6 \times 10^{19} \text{ 1/cm}^2\text{.s}. \tag{4.1.4}$$

Assume every photon creates an electron-hole pair, then the rate the carriers are created is,

$$G = N_{ph}/t = 4.6 \times 10^{23}\ 1/cm^3.s, \tag{4.1.5}$$

where t is the thickness of the absorption depth of the light in the sample. The rate of carrier generation within the switch volume is given by the following dynamic equation

$$\frac{dn_e}{dt} = \frac{dn_h}{dt} = G - \frac{n_e}{\tau} \tag{4.1.6}$$

where τ is the carrier recombination time. At peak photocurrent, the carrier generation is in steady state, therefore we have

$$\frac{dn_e}{dt} = \frac{dn_h}{dt} = G - \frac{n_e}{\tau} = 0 \tag{4.1.7}$$

$$\tau = n/G \tag{4.1.8}$$

The electron density is given by

$$J_p = qvn. \tag{4.1.9}$$

Substitute (4.2) in (4.9), we have the peak carrier density

$$n = J_p/qv = 3.1 \times 10^{15}\ 1/cm^3. \tag{4.1.10}$$

From (4.5) and (4.10), we can find the carrier recombination time

$$\tau = n/G = 6.7 \times 10^{-9}\ s = 6.7\ ns. \qquad (4.1.11)$$

This estimated lifetime is much shorter than the pulse width of the ArF excimer laser, indicating that the switch speed was limited by the laser.

D. Trigger Gain

We can also find the trigger gain of the 10 μm switches, which is defined as the ratio of the electrical pulsed energy switched to the load, E_{el}, to the optical energy of the laser pulse incident to the area between the electrodes, E_{op}, This area is $A = 3.2 \times 10^{-3}$ cm^2, thus

$$E_{op} = A/S = 0.91 \times 10^{-3}\ mJ = 0.91\ \mu J. \qquad (4.1.12)$$

Assuming square current pulse with pulse-width T = 30 ns, then from (4.1), we have

$$E_{el} = I^2 R_L T = 4.3\ \mu J. \qquad (4.1.13)$$

Therefore the trigger gain G_S of the switch is

$$G_S = E_{el}/E_{op} = 4.7. \qquad (4.1.14)$$

This gain is not high comparing to some other photoconductive semiconductor switches. For GaAs switch operating in lock-on mode, gain of 10^5 has been reported[54]. However, that switch was operated in non-linear mode (lock-on mode), so that the current pulse was

much longer. Besides, their material was single crystal. As we know, if the current pulse lasts longer, then more energy can be delivered to the load. In our case the current pulse was short and the switches operated in a linear mode. In order to get high gain, operating at nonlinear mode is necessary, such as lock-on mode and avalanche mode, but as a trade-off the switching speed will be sacrificed.

Also, the quantum efficiency of poly SiC was also expected to be relatively low. The quantum efficiency of the initial photocurrent is determined by the probability that the electron-hole pair will escape its mutual coulomb field. In most high-mobility semiconductors this probability is essentially 100%. In low-mobility material, however, the situation is quite different, and "geminate" recombination of electron-hole pairs can produce a significantly lower quantum efficiency[55].

E. Switching Efficiency

For most applications, a figure of merit called the "closing switch efficiency," or more commonly "switching efficiency," η_{sw}, is defined as the ratio of the peak voltage delivered to the load (V_L) to the peak voltage that would be delivered (V_{max}) if the switch were an "ideal" closing switch (i.e., zero on-state resistance, infinite off-state resistance). That is

$$\eta_{sw} = V_L / V_{max}. \qquad (4.1.15)$$

In our test circuit Figure 3.5, $V_{max} = V_C$, and $V_L = [R_L/(R_L + R_{on})]V_C$. Thus we have

$$\eta_{sw} = R_L/(R_L + R_{on}). \qquad (4.1.16)$$

The highest switching efficiency we obtained was

$$\eta_{sw} = R_L/(R_L + R_{on}) = 50/(50 + 46) = 52\%. \quad (4.1.17)$$

Higher switching efficiency of 86% was reported for 6H-SiC photoconductive switch[33]. In their case, single crystal was used. In our case, being polycrystalline material, our SiC samples have low mobility and the electrons in the sample experience strong scattering. Thus its on-state resistance is relatively higher, causing relatively lower switching efficiency. This is the disadvantage of polycrystalline material used for photoconductive switch.

F. Single Strip Gap Switches

Investigation of the single strip gap switches gave similar results. The switch speed and breakdown field were about the same as that of the interdigitated patterned switches. The photocurrent, however, was much lower, because of the small channel widths of the switches. A switch with 200 μm gap spacing could hold off 1000 V. Due to the limitation of the equipment, we did not go further. This result indicates that if we make large switch geometry, very high voltage and power could be switched by SiC switch. Therefore, practical power switching devices with high hold-off voltage and operating at high speed can be made from the poly 3C-SiC material.

4.1.2 The Dependence of The Performance on The Applied Bias

The dependence of the switch performance on the applied bias was investigated as follow. Under a fixed laser power and a repetitive rate, the applied voltage was increased gradually. At the same time, the photocurrent, switch off-state resistance, and on-state resistance were measured. To measure the switch breakdown voltage, the bias was

increased until breakdown occurred. At this time the reading of the voltmeter dropped to a very small value. Figure 4.4-6 shows the dependence of the off-state and on-state resistance, and peak photocurrent on the voltage, respectively. Figure 4.7-11 give more results which were obtained from different switches. Before discussing the results, one point need to be made clear. The laser power was not constant, it could fluctuate up to 20 percent. Corresponding fluctuation of the photocurrent pulse was observed. Thus the figures give roughly average values. Despite of that, all those figures have the following common features:

1. The switch on-state resistances are much smaller than the off-state resistances.
2. The peak photocurrent increases linearly with the applied voltage at low voltage.
3. When the voltage increases to a certain point, which we call critical point, the photocurrent stop increases linearly with the voltage, instead, it tends to be saturated.
4. After the critical point, the on-state resistance increases with the applied voltage. The critical point is different from switch to switch.
5. The off-state resistance decreases with the applied voltage after certain point.

We can conclude that at low voltage, the switches perform like conductor when optically activated, because the current increases linearly with voltage. At high voltage, however, the switches stop responding linearly to the applied bias. We attribute the current saturation to the saturation of the carrier drift velocity. The current density is determined by

$$J = q\,nv, \tag{4.1.18}$$

where q is electron charge, n is carrier density, and v is carrier drift velocity, or the decrease of the carrier mobility. It is apparent that when v approaches saturation, so does the current. As can be seen from Figure 4.4, the saturation voltage is about 170 V. Given

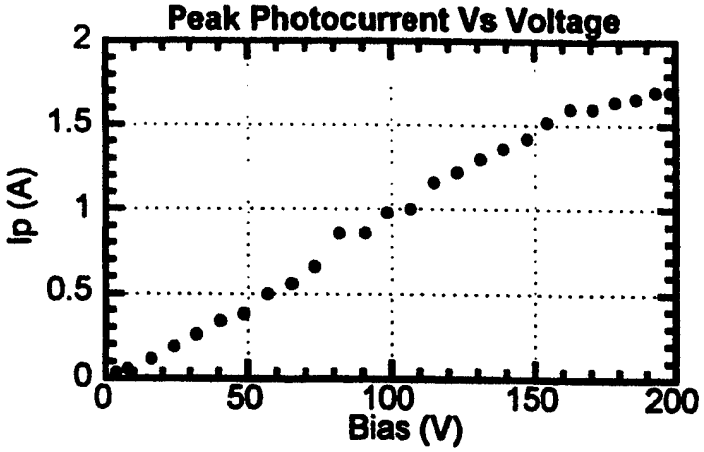

Fig. 4.4: The dependence of peak photocurrent on the bias applied on the switch

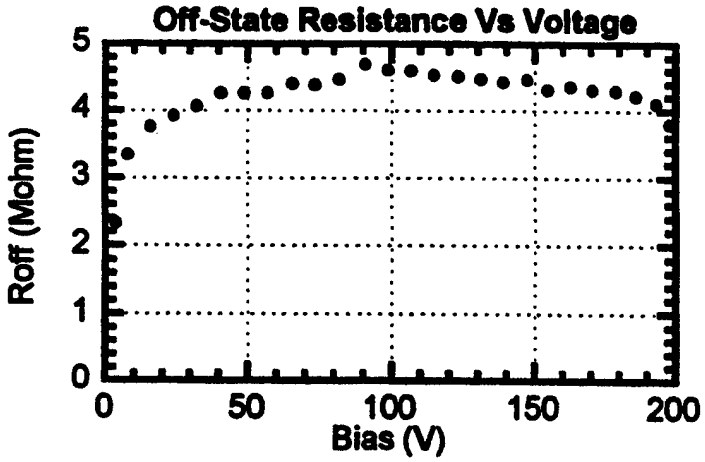

Fig. 4.5: The dependence of off-state resistance on the bias applied on the switch

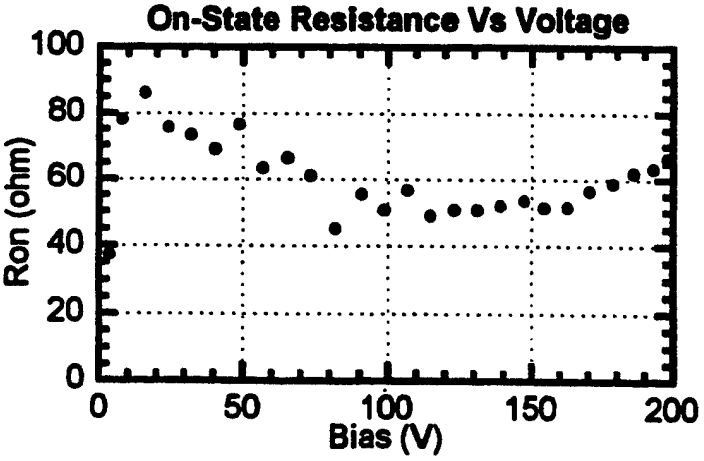

Fig. 4.6: The dependence of on-state resistance on the bias applied on the switch

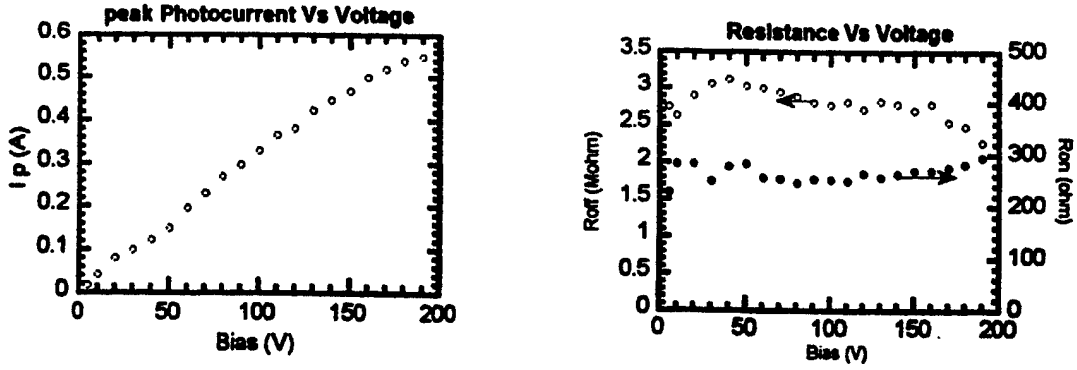

Fig. 4.7: Sample 1. Electrode gap: 10 μm.

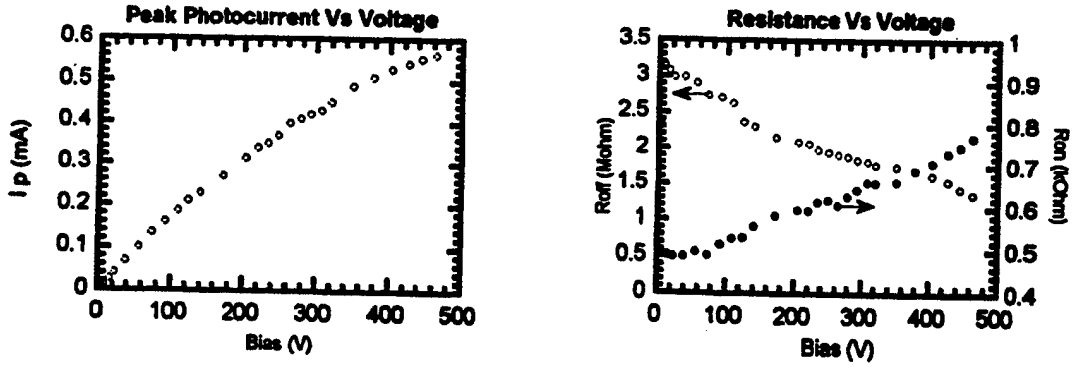

Fig. 4.8: Sample 2. Electrode gap: 70 μm.

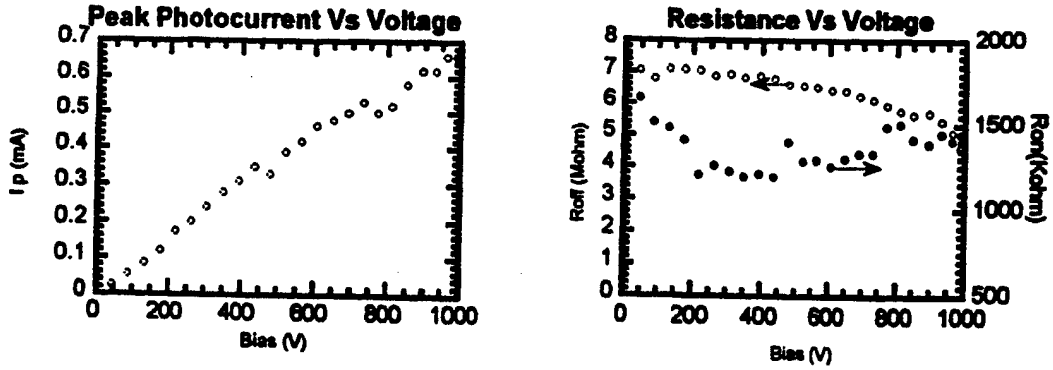

Fig. 4.9: Sample 3. Electrode gap: 200 μm.

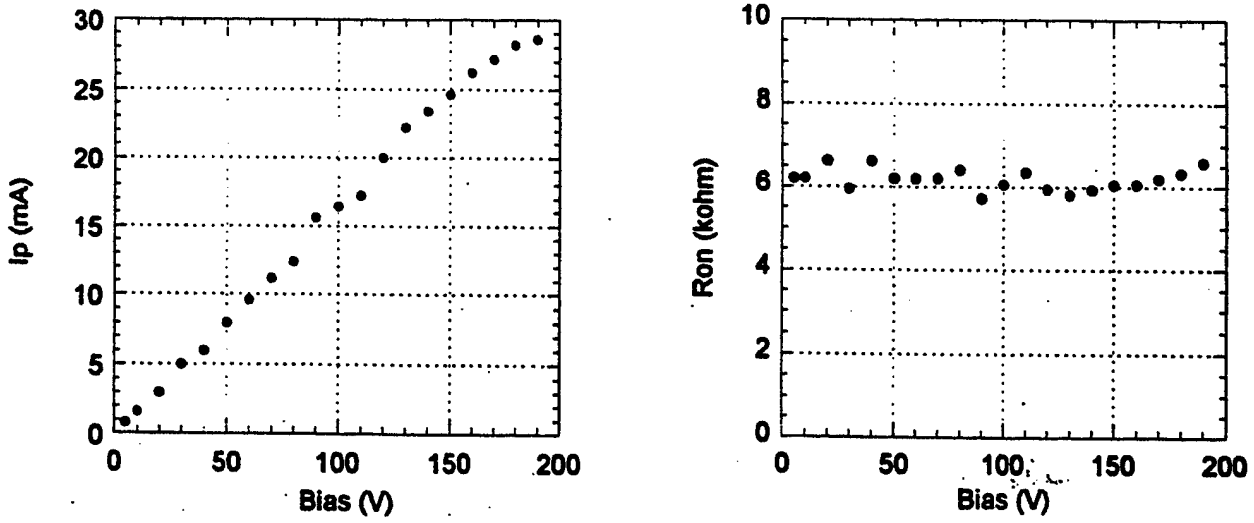

Fig. 4.10: Sample 4. Electrode gap: 10 μm.Light source: ArF excimer laser.

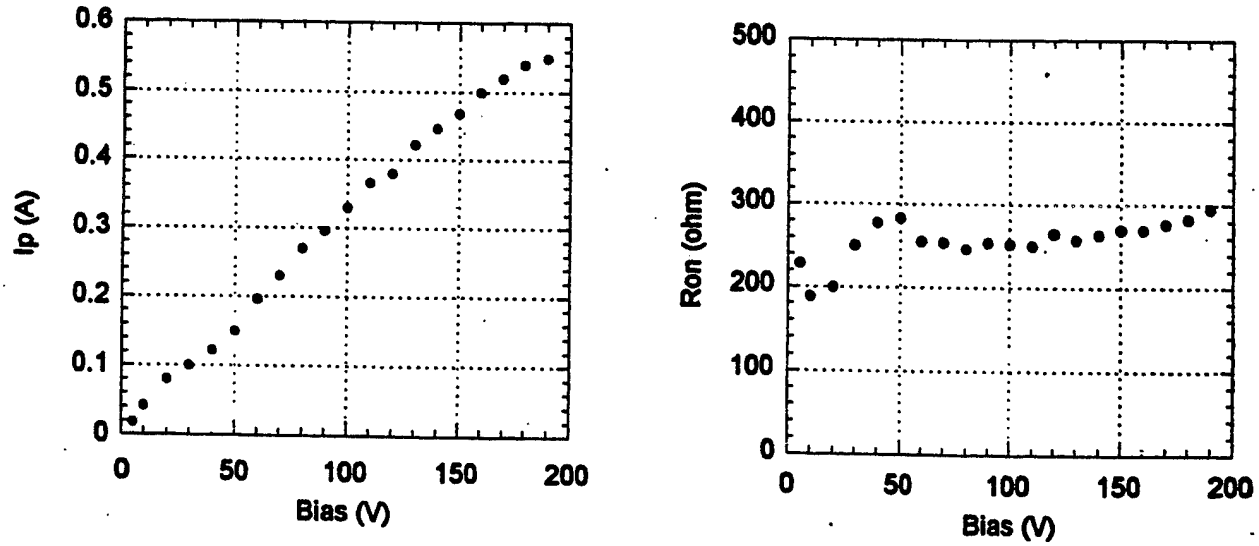

Fig. 4.11: Sample 5. Electrode gap: 10 μm.Light source: XeCl excimer laser.

the saturated electron drift velocity, $v \sim 2 \times 10^7$ cm/s, and the switch gap, 10 μm, we have the low field mobility of the material, $\mu \sim 120$ cm^2/V.s, which is a reasonable value for poly SiC.

The increase of the switch on-state resistance with applied voltage was also caused by the carrier velocity saturation. Since resistance is inversely proportional to the conductivity or

$$R_{on} \propto 1/\sigma = 1/q\mu n, \qquad (4.1.19)$$

and $v = \mu E$, where E is the electric field in the switch, we have

$$R_{on} \propto E/q \qquad nv = (1/q\, nvL)V, \qquad (4.1.20)$$

where L is the switch gap spacing. Therefore, when the velocity approaches saturation, the resistance increases with the applied voltage.

The decrease of the off-state resistance with the applied voltage might be caused by the crystalline grain boundaries within the material. It is unlikely that the resistance change happened inside the crystalline grains, because of the high breakdown field and wide band gap of 3C-SiC. Figure 4.12 gives one possible mechanism for this phenomenon. Due to the difference energy level structures in the grains and the boundaries, there is an energy barrier in the very thin boundary region or between the grains. When no bias is applied to the material, this barrier is the highest as shown in figure 4.12a. In this case, the carriers inside the material are of the most difficult to get through the barrier (only electrons are drown in the diagrams for simplicity). This results in the highest dark resistance of the material. When a voltage is applied, however, the barrier on one side decreases as shown

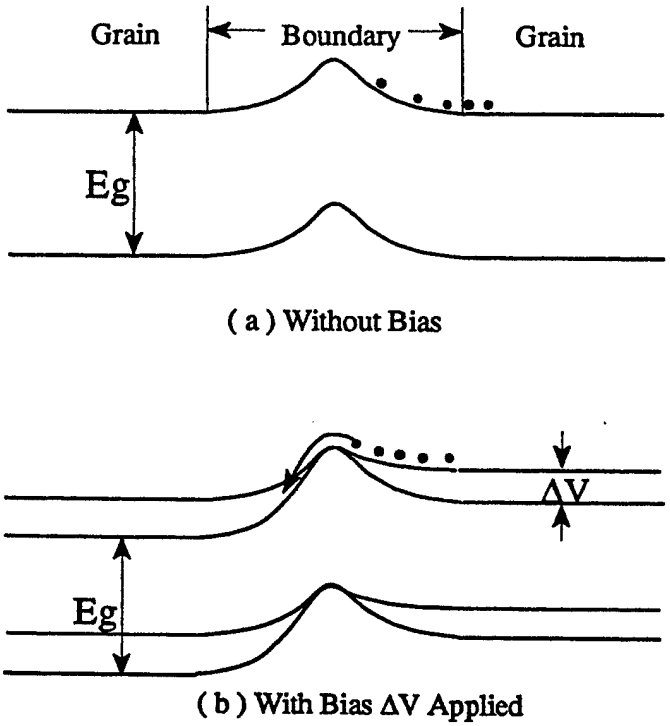

Fig. 4.12: The band diagram of the transition between the crystalline grains, and the change of the energy levels after a bias is applied

in Figure 4.12b. As a result, more carriers can pass the barrier, and the dark resistance decreases. Because of the complicated conditions in the poly SiC material, the details of the mechanism of the dependence of the dark resistance on the bias still remain to be understood.

From Figure 4.4, we can estimate the mobility of our poly 3C-SiC material. It can be seen that the current tend to saturate at voltage ~ 170 V. The saturation electron drift velocity of SiC is about 2.5×10^7 cm/s, from equation $v = \mu E$, we found the mobility of the poly 3C-SiC μ to be 144 cm^2 /V.s. Although it is just an approximation, this is a reasonable value for poly 3C-SiC. This is smaller than the mobility of single crystal SiC which has been measured at 300 - 750 cm^2 /V.s. In poly SiC material, because of the high

density of the boundaries of the crystallized grains, electrons experience strong scattering and the mean free path of electrons is much shorter than that in the single crystal. Therefore, the overall mobility of poly SiC is expected to be small.

4.1.3 The Dependence of The Performance on Laser Power Density

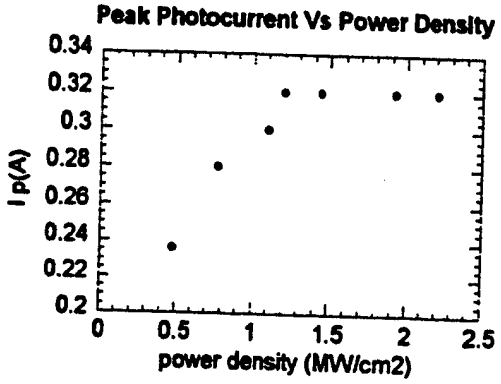

Fig. 4.13: Photocurrent as a function of the power density

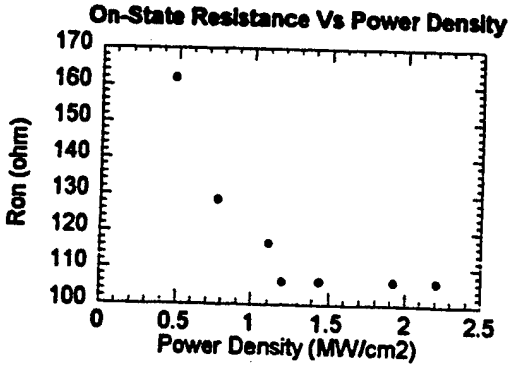

Fig. 4.14: Switch on-state resistance as a function of the power density

Figure 4.13 and Figure 4.14 show the dependence of the photocurrent and on-state resistance on the laser power density. The applied voltage on the switch was 50 V, and the

excitation light source was XeCl excimer laser. We can see from this figure that the photocurrent increases with the laser power density and saturates at about 1.1 MW/cm^2, and the on-state resistance decreases with the laser power density and finally stops decreasing. For all the tested switches, the photocurrents saturated at about the same laser power density, but the saturated photocurrents were different from switch to switch.

4.1.4 The Dependence of The Performance on Temperature

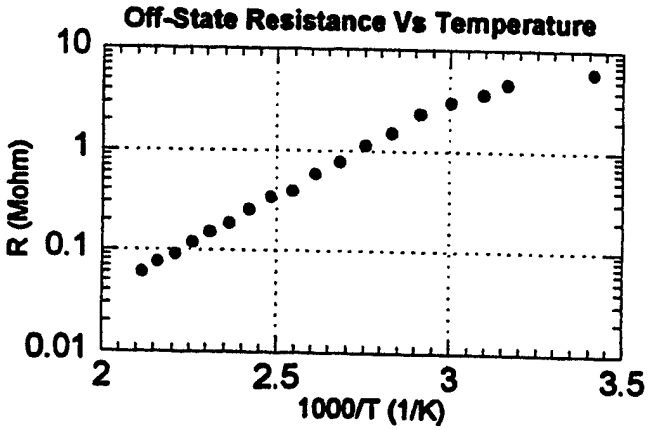

Fig. 15: Switch off-state resistance as a function of temperature

Temperature dependence of the performance of polycrystalline 3C-SiC switches was investigated. Figure 4.15 shows the dependence of the switch off-state resistance and the photocurrent on temperature. As can be seen, the off-state resistance decreases exponentially with the temperature. In the poly SiC materials, defect levels and impurity levels exist all over the band gap. When the temperature increases, the electrons and holes trapped in the shallow levels are very easy to be excited to the conduction band and valence band, respectively. Due to the high density of defects and impurity levels in the grains and boundaries, a large number of free carriers are created in the conduction and valence bands, resulting in a rapid decrease of the dark resistance of the material. At 100 °C, the dark resistance decreases to half of that at room temperature. From Figure 4.15, We can estimate the activation energy (E_a) of the poly SiC material. According to the Boltzmann law, the

electron density in the conduction band is given by

$$N = N_0 \exp[-(E_C - E_F)/kT] = N_0 \exp(-E_g/kT), \qquad (4.1.21)$$

where N_0 is electron density at room temperature. From Figure 4.15, we can find that the activation energy is about 0.33 eV.

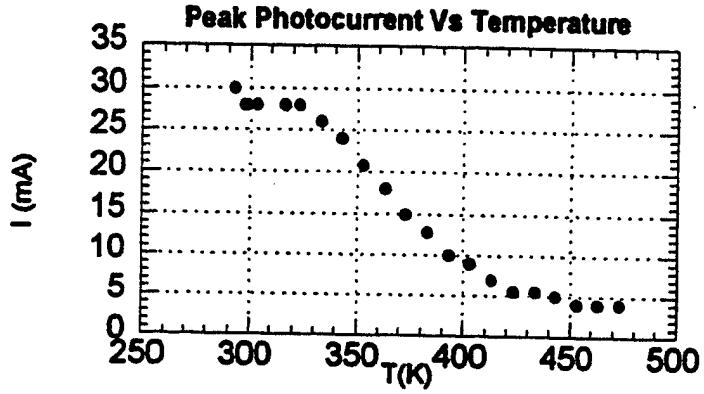

Fig. 16: Photocurrent as a function of temperature

The photocurrent also decreased with the temperature. At 100 °C, the photocurrent also decreased to half of that observed at room temperature as shown in Figure 4.16. Therefore polycrystalline 3C-SiC is not a suitable material for electronic devices operating at high temperature.

4.1.5 The Switch Breakdown Voltage for Different Contact Metalization

It was demonstrated in other materials that using different contact metalization systems for photoconductor switches resulted in different hold-off voltages[39, 56]. Choosing appropriate contact metals can reduce surface flashover effect. The following

contact metalization were used for our SiC photoconductive switches: Al, Ti/Al, Ni/Au, Cr/Au/Mo. Table 4.1 lists the breakdown voltage of the 10 μ gap switches. The table entries represent the best value of breakdown voltage obtained for each metalization system. The switches tested gave considerable difference in breakdown voltage within each particular contact type. The table shows a considerable variation in voltage standoff between different contact types. The Ni/Au contact system gave the highest breakdown.

Table 4.1: The switch breakdown voltage when using different metal contact and immersed in the air and fluorinert

breakdown voltage(V) \ material	Al	Ti-Al	Ni-Au	Cr-Au-Mo
in air	180	200	250	230
in fluorinert	445	450	560	465

The result indicates that the contact interface between the metallic conductors and the semiconductor is critical to the device voltage limitation. For different metalization, the field gradient at metal-semiconductor-dielectric triple-point is different, thus leading to different switch breakdown voltage. In addition the carrier-injection properties of the contacts can have a profound effect on the overall switch behavior[57-59].

Table 4.1 also lists the switch breakdown voltages when the switches were immersed in the liquid, fluorinert. The breakdown voltages in the liquid were more than doubled that in the air. This result reflects the surface flashover effect in another aspect for surface geometry device. In the medium with high dielectric strength, this effect is reduced. Peterkin, et al[60,61] investigated the temporal evolution of flashover in silicon utilizing high-speed imaging techniques. In their experiments, optical radiation was observed starting at the cathode as the flashover current rose. This radiation eventually traveled across the switch forming a filament.

4.1.6 The Photoresponse to Different Light Sources

Figure 4.17 shows the photocurrent pulses of a switch response to ArF laser and XeCl laser, Figure 4.18 and Figure 4.19 show the dependence of peak photocurrents and on-state resistances on applied voltage for both lasers. The results indicate that much higher photocurrent was obtained when using XeCl laser than using ArF laser, about 20 times, while the switch on-state resistance was lower when using XeCl laser than using ArF laser. This can be explained as follow:

1. The XeCl laser is relatively stronger. The pulse energy of XeCl laser is 138 mJ while that of ArF laser is 50 mJ. Thus XeCl laser generates more carriers.

2. XeCl laser creates photons more effectively. The wavelength of XeCl laser is longer than that of ArF laser. The former is 308 nm and the latter is 193 nm. Since the photon number is $P_O / h\nu = P_O \lambda / hC$, where P_O is the power of the light source and C is the speed of light, if the powers of both laser were the same, XeCl laser output more photons. Assuming each photon creates one electron-hole pair, then XeCl laser create more carriers in SiC material, resulting higher photocurrent.

3. The carriers experience stronger scattering when ArF laser is used. If the photon energy exceeds the threshold for photoconduction (the band gap in an intrinsic semiconductor) by an amount greater than the thermal energy kT, the excess energy is imparted to the electron-hole pair in the form of kinetic energy. At higher energy, the scattering is stronger, so the

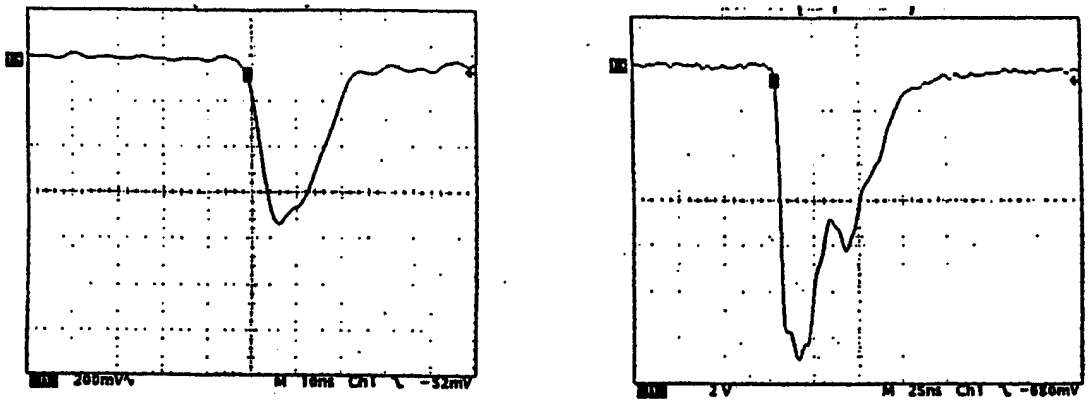

Fig. 4.17: The photocurrent pulses obtained from a switch of 10 μm gap while activated by a XeCl excimer laser and an ArF excimer laser.

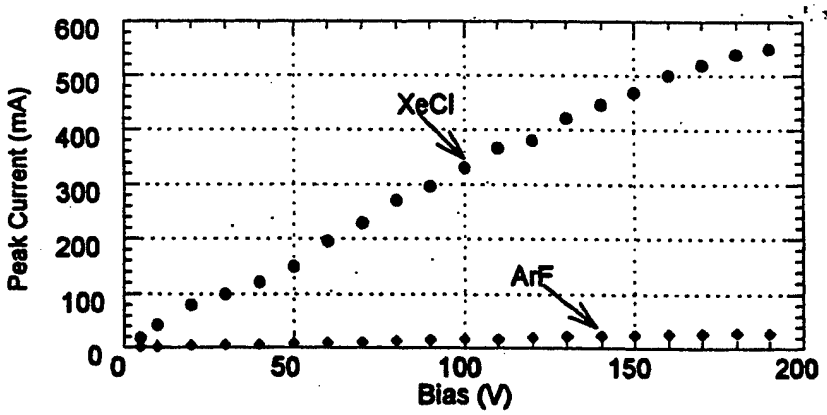

Fig. 4.18: The dependence of the photocurrent from a switch of 10 μm gap on voltage while activated by a XeCl excimer laser and an ArF excimer laser.

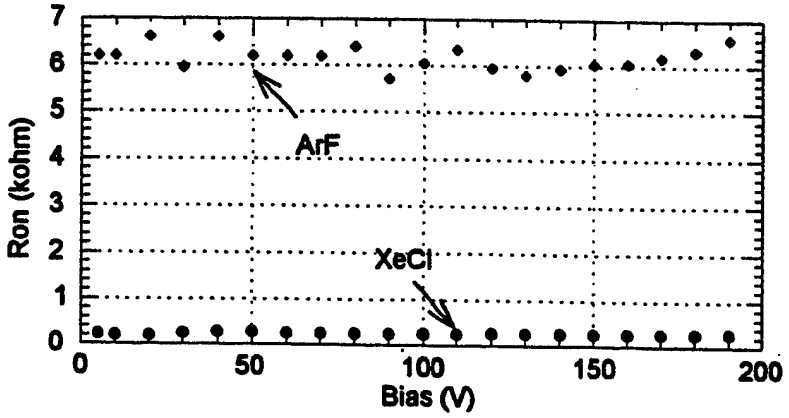

Fig. 4.19: The dependence of the on-state resistance of a switch of 10 μm gap on voltage while activated by a XeCl excimer laser and an ArF excimer laser.

mobility of the free carriers will be lower[62]. Since ArF laser creates more excess energy for the free electrons and holes, the mobility is lower in this case. Thus the on-state resistance and the photocurrent of the switch are lower when ArF laser is used.

4. The absorption depth of ArF laser in SiC is smaller. The scattering is stronger if the density of electron-hole pair is higher. At high carrier concentrations, hole-electron scattering limits the mobilities of electrons and holes, and thus decrease the switch efficiency and the photocurrent. Although electron-electron and hole-hole scattering do not change the net momentum of the electron and hole distributions, electron-hole scattering, however, can alter the net moneta of both the electron and hole distributions, and thus decrease the mobilities for both carriers [63]. Again, Since the wavelength of ArF laser is shorter, the corresponding absorption depth in SiC is also shorter. Thus the temporary conductive layer in the switch is thinner when it is illuminated. If the two lasers output the same power, then the density of generated electron-hole pair is higher when the light source is ArF laser, assuming each photon generates an electron-hole pair. Thus the scattering of the electron-hole pairs is stronger when ArF laser is used, and the momentum loss of electrons and holes is more. Therefore, the photocurrent is smaller.

4.1.7 The Photoresponse To The Light From Xe/Hg Lamp

When the switch was illuminated by Xe/Hg lamp, very small photocurrent was observed. The lamp output spectrum consists of continuous wavelength from ultra violet to infrared light. The spectrum experiment of the switch showed that the switch not only responded to UV light, which has higher energy than the band gap but also to the infrared light, which has lower energy than the band gap. This result indicates that there are defect states in the band gap including deep and very shallow states. The photoresponse was slow. On an oscilloscope, it was observed that the photocurrent pulse rose fast but decayed very slowly. The fall-time of the pulse was several seconds. This fall-time is much longer than the fall-time when excimer laser was used (nanoseconds), and even much

longer than the carrier lifetime of single crystal 3C-SiC. We suspect that at low optical power, electron-hole recombination is not the main mechanism of carrier recombination in our poly SiC material. The defect and impurity states in the band gap play an important roll. The number excited from defect and impurity states in the band gap is comparable to the carrier number from band-to-band transition. Thus the carriers are not necessary paired to be electron-hole pairs. The recombination through these states is relatively slower than electron-hole recombination. Further, amongst the defect states there are many trap centers. The re-emission of electrons and holes from the centers makes the decay slower. As mentioned in section 4.1.1 where laser is the light source, when the photocurrent approaches to zero, the decay is also very slow. We believe the mechanism there is the same. This slow decay was also observed for 6H-SiC material by other researchers. The exact cause of the observed slow decay is, however, not completely understood at this time.

4.2 SWITCHES FABRICATED ON SINGLE CRYSTAL 3C-SIC SAMPLES

The results for single crystal 3C-SiC switches were not as good as that for poly 3C-SiC PCSS. Both the boron doped and unintentionally doped 3C-SiC single crystal materials suffered the same problem, that is low resistivity. Due to the low resistivity of the materials, the switches could not hold off high voltage. Only several volts could be applied on these devices. For this reason, the boron doped and unintentionally doped SiC materials could not be used to make practical power switching devices. This widths of the photocurrent pulses obtained from those switches were about the same as that obtained from the polycrystalline 3C-SiC switches. Thus the switching speed of those switches was also limited by the laser pulse. Figure 4.20-22 show photocurrent pulses measured from a unintentionally doped 3C-SiC switches with and without bias. We found that even without bias, photocurrent pulse was measured as shown in Figure 4.20. That is photovoltaic effect. Since the electrodes are not only symmetrical but also mixed together (interdigitated

pattern), this is yet to be understood. This photovoltaic effect was also observed by other researchers[33, 34] for 6H-SiC with single gap pattern. When the applied voltage was increased in positive direction, the photocurrent increased. The current was the addition of the photovoltaic signal and the photoconductive signal as shown in Figure 4.21. When the voltage was increased in the negative direction, the photocurrent was the subtraction of the photovoltaic signal to the photoconductive signal as shown in Figure 4.22.

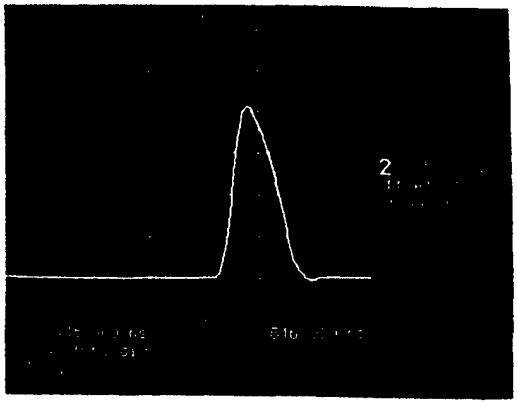

Fig. 4.20: Current pulse obtained from unintentionally doped 3C-SiC switch with zero bias

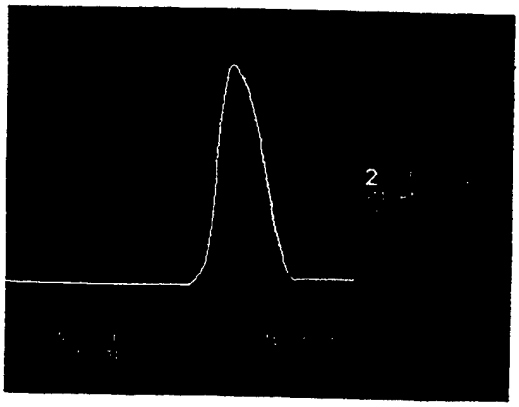

Fig. 4.21: Current pulse obtained from unintentionally doped 3C-SiC switch with positive bias 4.0 V

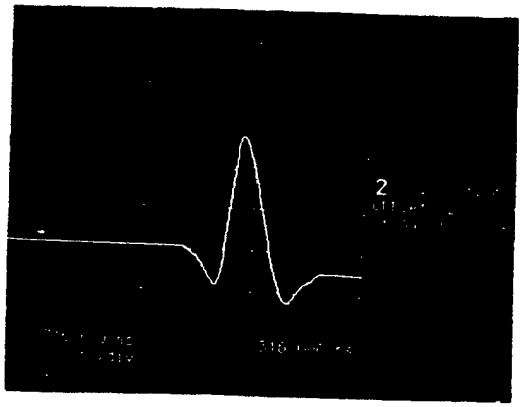

Fig. 4.22: Photocurrent pulse obtained from unintentionally doped 3C-SiC switch with negative bias -4.0 V

CHAPTER V

CONCLUSIONS AND RECOMMENDATIONS

5.1 CONCLUSIONS

3C-SiC is a potential material for power switching devices because of its favorable properties. Photoconductive switch fabricated from 3C-SiC has numerous applications. Study of the performance of the switch has technological and economical significance. The first 3C-SiC photoconductive switches were fabricated in this laboratory from the following three types of the material: unintentionally doped and boron doped single crystal, and polycrystalline material. The switch performances were investigated using ArF and XeCl excimer lasers. Best results were obtained from the switches fabricated from the polycrystalline 3C-SiC material. The material has the desired dark resistivity (1MΩcm) and the switches had an ideal off-state. For the 10 μm gap switches, the current leakage was only 22 μA at 100 V. The highest peak photocurrent obtained was 1.7 A, which corresponds to a current density of 10 kA/cm^2. The lowest on-state resistance of the switches was 45 Ω while the off-state resistance was about 4.5 MΩ, thus the ratio of off-state resistance to on-state resistance, R_{off}/R_{on}, was 10^5. The highest breakdown field of the switches was 250 kV/cm, which is the highest breakdown field reported for lateral photoconductive semiconductor switches, and the corresponding was 250 V. The hold-off voltage of the switch was limited by the surface flashover effect. When using different metallization contact systems for the electrodes, the breakdown voltages of the switches were different. At low field the photocurrent increases linearly with the applied bias, but at high field it saturates because of the saturation of the electron drift velocity in the 3C-SiC material. The switches have a much shorter carrier lifetime than that reported for single crystal 3C-SiC material. The shortest width of photocurrent pulse observed was 15 ns, which was limited by the excitation laser pulses and the testing circuit. We believe that with a faster light source and an appropriate circuit configuration the switch can operate in

subnanosecond regime.

Investigation of larger gap switches shows that high hold-off voltage can be reached by increasing the separation of the electrodes of the switch. A switch with 200 μm electrodes separation could hold off more than 1000 V bias. This result indicates that practical photoconductive switches with large power handling capability can be fabricated from 3C-SiC material.

The switching efficiency of our poly 3C-SiC switches was 52%, and the trigger gain was 4.7. One remedy to increase the switching efficiency is to use single crystal 3C-SiC with high resistivity. The switch performances degraded as temperature increased because of the high density of grain boundaries and other type defects. Thus the switches can not be used for high temperature application. The solution for that is also the use of single crystal 3C-SiC.

5. 2 SUGGESTIONS FOR FUTURE WORK

There are a lot of work need to be done to make practical 3C-SiC photoconductive switch used for large pulsed power systems and to understand its performance. For our polycrystalline 3C-SiC switches we only used a very thin layer of the material to switch power from the source to the load because of the short absorption depths of the excitation sources. To utilize a thicker layer, laser with longer wavelength need to be used. XeF excimer laser, whose wavelength is 368 nm, is a candidate for a short run in this lab. The absorption depth of XeF excimer laser is 20 times longer than that of XeCl excimer laser. In a long run, GaN blue laser is a perfect choice. The absorption depth is much longer. Since it can be made very compact and is easy to integrate, laser array can be developed to obtain desired power for the switch, so that the switch can deliver high power. Besides, with the help of mode-lock and optoelectronic technology, the laser pulse can be made extremely short (picosecond level). Thus the switch speed will not be limited by the optical source.

To measure the exact switch speed and the carrier lifetime of SiC material, an innovative test technique need be employed. The use of transmission line can eliminate the effects from the circuit such as parasitic capacitors and inductors.

Practical photoconductive switch could not be fabricated from our single crystal material due to its low resistivity. This problem could be overcome by ion bombardment followed by rapid thermal annealing. An ideal ion source is that only deep level states are created in the bandgap after the bombardment. The performance of switch fabricated from single crystal 3C-SiC with high resistivity should be better from polycrystalline 3C-SiC. High hold-off voltage and power handling capability should be able to reached. Higher switching efficiency and trigger gain should also be reached because the mobility of single crystal is higher than polycrystalline material. The switch will be able to operate at high temperature because there is no grain boundary effect in single crystal material.

REFERENCES

[1] D. H. Auston, *Appl. Phys. Lett.*, Vol. 26, (1975), p. 101.

[2] G. Mourou, et al, *Appl. Phys. Lett.*, Vol. 35, (1979), p. 492.

[3] C. H. Lee, "Picosecond Optoelectronic Devices," Academic Press, Inc, Orlando, 1984.

[4] D. H. Auston and P. R. Smith, *Appl. Phys. Lett.* Vol. 43, (1985), p. 631.

[5] E. A. ChuaChard, et al, *Appl. Phys. Lett.* Vol. 47, No. 12, (1985), p. 1293.

[6] P. -T, Ho, et al, *IEEE Trans. Electron Devices*, Vol. 37, (1990), p. 2517.

[7] A. Rosen, et al, "High-Power Optically Activated Solid-State Switches", Boston: Artech House, 1994.

[8] C. H. Lee, et al, *Appl. Phys. Lett.* Vol. 30, (1977), p. 84.

[9] R. S. Wagner, et al, *IEEE Trans. Nuclear Science*, Vol. 33, No.1, (1986), p. 250.

[10] C. L. Wang, et al, *Rev. Science Instruments,* Vol. 57, (1986), p. 2182.

[11] J. Agostinelli, et al, *Appl. Phys. Lett.*, Vol. 35, (1979), p. 731.

[12] V. K. Mathur, et al, *IEEE J. Quantum Electron.* QE-18, (1982), p. 205.

[13] G. Mourou, et al, *Appl. Phys. Lett.,* Vol. 36, (1980), p. 623.

[14] G. M. Loubriel, *Proc. 6th IEEE Pulsed Power Conf.* Arlington, VA, 1987, p. 145.

[15] F. J. Zutravern, *Proc. 6th IEEE Pulsed Power Conf.* Arlington, VA, p. 577.

[16] R. A. Petr, et al, *Conf. Proc. 6th Symp. Electromagnetic Launcher Technology,* Austin, TX, 1992.

[17] R. A. Petr, et al, *Proc. 6th IEEE Pulsed Power Conf.* Arlington, VA, 1987, p.608

[18] C. H. Lee, *IEEE J. Quantum Electronics,* Vol. QE-16, No. 3, (1980), p. 277.

[19] W. C. Nunnally, et al, *Appl. Phys. Lett.,* Vol. 44, (1984), p. 980.

[20] G. Loubriel, et al, *Proc. 18th IEEE Power Modular Symp.* Hilton Head, SC, 1988, p. 312.

[21] M. S. White, et al, *Opt. Commun.* Vol. 43, (1982), p. 53.

[22] C. H. Lee, "Picosecond Optoelectronic Devices," Academic Press, Orlando, 1984, p. 379.

[23] W. C. Nunnally, et al, *Appl. Phys. Lett.* Vol. 44, No.10, (1984), p. 980.

[24] R. M. Goeller, et al, *Proc. 6th IEEE Pulsed Power Conf.* Arlington, VA, 1987, p. 157.

[25] A. Rosen, et al, *IEEE Photonic Tech. Lett.* Vol. 2, No. 7, (1990), p. 525.

[26] H. Zhao, et al, *Optically Activated Switching II, SPIE Proc.* Vol. 1632, Las Angeles, CA, 1992, p. 274.

[27] R. P. Brinkmann, et al, *IEEE Trans. Electron Devices,* Vol. 38, No. 4, (1991), p. 701.

[28] G. Loubriel, et al, *IEEE Trans. Electron Devices,* Vol. 38, No. 4, (1991), p. 692.

[29] F. J. Zutavern, et al, *IEEE Trans. Electron Devices,* Vol. 38, No. 4, (1991), p. 696.

[30] P. A. Glasow, *Springer Proc. in Phys.* "Amorphous and Crystalline Silicon Carbide and Related Materials, Berlin," 1988, p. 13.

[31] J. A. Powell, et al, *Springer Proc. in Phys.* "Amorphous and Crystalline Silicon Carbide and Related Materials," Berlin, 1988, p. 2.

[32] S. Saddow, et al, *9th Annual IEEE Sarnoff Symp. Digest,* 1993.

[33] P. K. Cho, et al, *J. Appl. Phys.* 77, No. 4, (1995), p. 1591.

[34] J. Coleman, G. Harris, *MRS 1996 Spring Meeting,* San Francisco, CA, 1996.

[35] J. A. Edmond, et al, "High Temperature Implantation of Single Crystal Beta Silicon Carbide Thin Films," North Carolina State University.

[36] V. Valilov, and N. A. Ukhin, "Radiation effects in Semiconductors and Semiconductor Devices." Plenum, New York, 1977.

[37] C. H. Lee, "Picosecond Optoelectronics Devices", Academic Press, Orlando, 1984, p. 393.

[38] W. C. Nunnally, et al, "Photoconductive Switches, Los Alamos National Laboratory Report," Las Alamos, NM, April 1983.

[39] G. M. Loubriel, et al, "Conf. Elec. Insulation and Dielectric Phenomena," 1988, p. 430.

[40] W. C. Nunnally, et al, "Photoconductive Switches, Los Alamos National Laboratory Report," Las Alamos, NM, April 1983. book, p. 38.

[41] C. H. Lee, "Picosecond Optoelectronics Devices", Academic Press, Orlando, 1984, p. 192.

[42] R. A. Smith, "Semiconductors," 2nd ed. Cambridge Univ. Press, London, 1978.

[43] P. R. Smith, et al, *Appl. Phys. Lett.* Vol. 39, (1981) p. 739.

[44] C. Erginsoy, *Phys. Rev.* Vol. 79, (1950), p. 1013.

[45] K. K. Diogu, et al, *3rd Intl. High Temp. Elec. Conf.* Albuquerque, NM, 1996.

[46] G. L. Harris, et al, "Proc. 5th Conf. Silicon Carbide and Related Materials," Washington, DC, 1993, p. 715.

[47] W. Sah, et al, *Springer Proc. in Phys.* "Amorphous and Crystalline Silicon Carbide and Related Materials II," 1988, p. 88.

[48] Y. Chinone, et al, *Springer Proc. in Phys.* "Amorphous and Crystalline Silicon Carbide and Related Materials II," 1989, p. 198.

[49] W. J. Choyke, et al, *J. Appl. Phys.* Vol. 64, No. 6, (1988), p. 3163.

[50] A. Solangi and M. I. Chaudhry, *J. Mater. Res.* Vol. 7, No. 3, (1992), p. 539.

[51] H. Okumura, et al, *Springer Proceedings in Physics, Vol. 43*, "Amorphous and Crystalline Silicon Carbide and Related Materials II," Berlin, 1989, p. 94.

[52] S. Saddow, et al, *Optically Activated Switching III*, Proc. SPIE, Los Angeles, 1993, p. 110.

[53] S. Saddow, et al, "Proc. 5th Intl. Conf. Silicon Carbide and Related Materials," Washington, DC, 1993, p. 573.

[54] F. Zutavern, et al, *Proc. Optically Activated Switching II*, SPIE Vol. 1632, 1992, p. 152.

[55] C. H. Lee, "Picosecond Optoelectronics Devices", Academic Press, Orlando, 1984, p.73.

[56] R. Feuerstien, and B. Senitzky, *Proc. 7th IEEE Pulsed Power Conf.* 1989, p. 358.

[57] S. E. Thompson, and F. A. Lindholm, *IEEE Trans. on Electron Devices*, Vol. 37, (1988), p. 2542.

[58] D. C. Stoudt, et al, *IEEE Trans. on Electron Devices*, Vol. 37, (1990), p. 2478.

[59] R. P. Brinkham, et al, IEEE Trans. on Electron Devices, Vol.38, (1991), p. 701

[60] F. E. Peterkin, et al, *IEEE Trans. on Electron Devices*, Vol. 37, (1990), p. 2459.

[61] S. H. Nam and T. S. Sudarshan, *IEEE Trans. on Electron Devices*, Vol. 37, (1990), p. 2466.

[62] K. Seeger,"Semiconductor Physics." Springer-Verlag, Berlin and New York., 1973.

[63] J.M. Dorkel, and P. Leturcq, *Solid-State Electron.* Vol. 24, (1981), p.821.